



Initial ASME Graphite Code Rule Analysis on Simplified and Full Assessments Within BPVC Subsection HHA

August 2022

Andrea Mack
Idaho National Laboratory



*INL is a U.S. Department of Energy National Laboratory
operated by Battelle Energy Alliance, LLC*

DISCLAIMER

This information was prepared as an account of work sponsored by an agency of the U.S. Government. Neither the U.S. Government nor any agency thereof, nor any of their employees, makes any warranty, expressed or implied, or assumes any legal liability or responsibility for the accuracy, completeness, or usefulness, of any information, apparatus, product, or process disclosed, or represents that its use would not infringe privately owned rights. References herein to any specific commercial product, process, or service by trade name, trade mark, manufacturer, or otherwise, does not necessarily constitute or imply its endorsement, recommendation, or favoring by the U.S. Government or any agency thereof. The views and opinions of authors expressed herein do not necessarily state or reflect those of the U.S. Government or any agency thereof.

Initial ASME Graphite Code Rule Analysis on Simplified and Full Assessments Within BPVC Subsection HHA

**Andrea Mack
Idaho National Laboratory**

August 2022

**Idaho National Laboratory
Advanced Reactor Technologies
Idaho Falls, Idaho 83415**

<http://www.art.inl.gov>

**Prepared for the
U.S. Department of Energy
Office of Nuclear Energy
Under DOE Idaho Operations Office
Contract DE-AC07-05ID14517**

Page intentionally left blank

INL ART Program


Initial ASME Graphite Code Rule Analysis on Simplified and Full Assessments Within BPVC

INL/RPT-68991

Revision 0

August 2022

Technical Reviewer: (Confirmation of mathematical accuracy, and correctness of data and appropriateness of assumptions.)

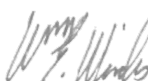


Joseph Bass

9/2/2022

Date

Approved by:



William E. Windes
ART Graphite R&D Technical Lead

9/2/2022

Date

Travis Mitchell for

Michael E. Davenport
ART Project Manager

9/2/2022

Date

Michelle Sharp

Michelle T. Sharp
INL Quality Assurance

9/2/2022

Date

ABSTRACT

The code rules created by the American Society of Mechanical Engineers (ASME) and the American Society for Testing and Materials (ASTM) present methodologies for conducting both simplified and full assessments to qualify nuclear grade graphite components for service within nuclear applications. This report explains the theory behind the statistical portion of the codes and describes the issues discussed in two stakeholder workshops on code rules pertaining to the simplified and full assessments specified in Subsection HH, Subpart A (HHA) of the ASME Boiler Pressure and Vessel Code (BPVC), Section III Division 5 (III-5). The original methodology for the full assessment was developed by Michael Hindley, who used a validation methodology to match the experimental average failure load of test specimens associated with various geometries to the calculated 50% probability of failure (POF) load in order to tune the grouping criteria parameters based on a root mean squared error (RMSE) penalty function. Hindley's work is discussed throughout the document.

The main findings from this report involve sensitivity studies that were performed to evaluate: the volume grouping criteria, the mesh size, and the threshold parameter effects on the POF and component acceptance decision. All three were found to affect the component qualification decision for components of structural reliability class 1 (SRC-1). Results from the sensitivity analysis are presented in the body of the report for graphite grade NBG-18. The results demonstrate that increases to the threshold parameter decreases the POF, that finer mesh sizes result in higher (more conservative) failure probabilities, and that smaller link volume requirements lead to higher failure probabilities. Results for the additional graphite grades of NBG-17, IG-110, 2114, and PCEA are included where applicable.

This report proposes a new validation study similar to the study performed for the previous code rules to tune the threshold, mesh size and the minimum link volume grouping criteria based on the results from multiple grades of graphite, including the super-fine grain graphite grades (< 50 microns) to micro-fine grain sized grades (< 2 microns). The tentative mechanical testing will be performed at three different laboratories to allow for estimates of between-laboratory testing variability. Unlike Hindley's validation method which attempted to match the average experimental load with the median values, the future study will attempt to match failures at lower percentiles, something that will be applicable to the structural reliability class probability of failure limit. The validation study will also apply the ASME methodology to specimens which have multi-axial stress states. Appropriate specimen geometries, specimen sizes, and test methods for measuring multi-axial stress states are all being investigated.

In addition to these major findings, this report also provides a background to the Weibull distribution, documents the 2020 workshop that was held to discuss the conservatism in the allowable stress calculated in the simplified assessment, documents issues found in the 2021 version of the full assessment's minimum link volume criteria that was based on fracture toughness.

CONTENTS

ABSTRACT.....	v
ACRONYMS.....	x
1. BACKGROUND.....	1
2. GRAPHITE.....	1
3. WEIBULL DISTRIBUTION.....	2
3.1 Description.....	2
3.2 Weakest Link Theory.....	6
3.3 Parameter Estimation.....	6
3.3.1 Maximum Likelihood Estimation.....	6
3.3.2 Least Squares Estimators.....	8
3.3.3 Method of Moment Estimators.....	8
3.3.4 Other Considerations.....	8
3.4 Basis for Use of Weibull Distribution.....	9
4. SIMPLIFIED ASSESSMENT.....	9
4.1 Method.....	9
4.2 2020 Workshop.....	10
4.2.1 Goodness of Fit Analysis.....	17
5. FULL ASSESSMENT.....	19
5.1 Method.....	19
5.2 Sensitivity Analysis Results Presented at the 2022 Workshop.....	20
5.2.1 Maximum Likelihood Estimation and the Threshold Parameter.....	20
5.2.2 Update Step and Shape Effect.....	21
5.3 Mesh Size Effects.....	23
5.4 Grouping Step.....	26
5.4.1 Weibull's Weakest Link Theory.....	26
5.4.2 Criteria.....	27
5.5 V_m Sensitivity Study Results.....	30
5.6 Other Considerations.....	35
6. VALIDATION.....	35
7. REFERENCES.....	39

FIGURES

Figure 1. Weibull distribution: fixed scale and threshold, varying shape parameter.....	3
Figure 2. Weibull distribution: fixed shape and threshold, varying scale parameter.....	3
Figure 3. Weibull distribution: fixed shape and scale, varying threshold parameter.....	4
Figure 4. POF as a function of threshold: NBG-18.	7
Figure 5. Comparison of MLE and lower bound distribution fits for NBG-18.	10
Figure 6. Comparison of POF from MLE and lower bound distribution based on SRC-1 limit for NBG 18.....	11
Figure 7. Zoomed in image of area of overlap for MLE and lower bound NBG-18 distributions.	12
Figure 8. Comparison of lower bound Weibull CDFs.	13
Figure 9. Average area of overlap between MLE and lower-bound distributions as a function of sample size.....	14
Figure 10. Variability in the area of overlap between MLE and lower-bound distributions as a function of sample size.	15
Figure 11. Comparison of MLE and lower-bound distribution fits for NBG-17.....	15
Figure 12. Comparison of MLE and lower-bound distribution fits for PCEA.	16
Figure 13. Comparison of MLE and lower bound-distribution fits for IG-110.	16
Figure 14. Goodness-of-fit plots.	17
Figure 15. Five distributions used in full assessment POF calculations: NBG-18.	21
Figure 16. Five distributions used in full assessment POF calculations: NBG-18, zoomed in.....	22
Figure 17. Component volume distributions.....	23
Figure 18. Component stress distributions vs. NBG-18 test data stress distribution.....	24
Figure 19. NBG-18: POF as a function of threshold and mesh size.	24
Figure 20. NBG-18: POF as a function of threshold and mesh size, zoomed in.	25
Figure 21. Step (4) from the 2019 and 2021 ASME BPVC versions.	27
Figure 22. Schematic defining the process zone parameters.	28
Figure 23. NBG-18: POF as a function of threshold and V_m , fine mesh.	31
Figure 24. PCEA: POF as a function of threshold and V_m , fine mesh.....	32
Figure 25. IG-110: POF as a function of threshold and V_m , fine mesh.	32
Figure 26. Comparison of lower-bound distributions used in POF calculations vs. component stress distribution for all grades of graphite.....	33
Figure 27. Comparison of group sizes in POF calculations.....	34
Figure 28. Boxplot of effective group volumes relative to V_m limit.....	34
Figure 29. Boxplot of effective group relative stress ranges vs. limit.	35

TABLES

Table 1. Goodness of fit statistics output.	18
Table 2. Weibull parameters associated with Figure 15 and Figure 16.	22
Table 3. Table of POF values as a function of original threshold, updated threshold and mesh size.	25
Table 4. Expanded version of Table 3 from [13].	29
Table 5. Table of previous validation work.	37

Page intentionally left blank

ACRONYMS

ASME	American Society of Mechanical Engineers
ASTM	American Society for Testing and Materials
BPVC	Boiler Pressure Vessel Code
CDF	cumulative distribution function
FEA	finite element analysis
GOF	goodness of fit
HTR	high-temperature reactor
MLE	maximum likelihood estimation
MOM	method of moment
NPP	nuclear power plant
NRC	Nuclear Regulatory Commission
PDF	probability density function
POF	probability of failure
Q-Q	quantile-quantile
SRC	structural reliability class

Page intentionally left blank

Initial ASME Graphite Code Rule Analysis on Simplified and Full Assessments Within BPVC Subsection HHA

1. BACKGROUND

Reactor designs capable of operating safely at temperatures 2 or even 3 times the operating temperatures of current light-water reactors are primarily enabled by the specialized materials proposed in these designs. High-temperature metallic alloys, ceramics, composites, and graphitic components are necessary for achieving these high-operating temperatures. However, these materials are not normally utilized within the nuclear field, and few rules or guidance have previously existed on how to utilize them for novel nuclear applications. That being said, over the last 20 years, the American Society of Mechanical Engineers (ASME) has been actively developing new rules governing the usage of these materials within nuclear applications.

The Boiler Pressure Vessel Code (BPVC) is primarily divided into sections, divisions, subsections, subparts, and articles. This report focuses exclusively on the graphite code rules contained within **Section III** (Rules for Construction of Nuclear Facility Components), **Division 5** (HTRs), **Subsection HH** (Class SN Nonmetallic Core Components), **Subpart A** (Graphite Materials), or Section III-5 HHA, for short. HHA is composed of different articles specifying code rules within General Requirements, Materials, Design, Testing, and other areas important to the design and safety of HTR construction. The information and discussion in this report primarily addresses specific code issues pertaining to **Article HHA-3000** (Design).

The USA's Nuclear Regulatory Commission (NRC) regulates the commercial nuclear power plants (NPPs) and nuclear material use in the United States. The NRC utilizes the ASME BPVC as an important tool for licensing and regulating questions of these commercial NPPs. As such, the NRC is considering the endorsement of HHA code rules for HTR graphite component designs (with some exceptions). This endorsement is expected in late 2022.

Finally, it should be noted that while ASME does not specifically require adherence to American Society for Testing and Materials (ASTM) standards for testing, qualification, and design code rules for graphite, it is an important consideration in the licensing and operational permissions granted to these commercial NPPs. A standardized test or qualification methodology from ASTM ensures that practices are consistent and precise. In this report, ASTM-D-7846 (Standard Practice for Reporting Uniaxial Strength Data and Estimating Weibull Distribution Parameters for Advanced Graphites) is important for both the Materials and Design articles in HHA.

2. GRAPHITE

Most of the code rules in Section III-5 HHA address the unique behavior and material properties of graphite. One of graphite's primary attributes is its brittle fracture behavior, which implies unstable crack propagation (unchecked crack propagation) through the component even at relatively low applied stress levels. Ductile fracture (stable crack propagation) occurs in readily deformable (malleable) materials and is characterized by the need for continuous addition of energy to propagate a crack through the material. Understanding graphite's unstable brittle fracture behavior requires determining the probabilities for crack propagation under all loads, as calculated via the applied stresses on the component as well as the material's inherent strength. One of the most common methods from predicting crack initiation and propagation is Weibull's weakest link theory. The weakest link theory states that a component's survival probability is the product of the survival probability of each volume element [3], where each volume element is assumed to be independent. The functional form of the survival probability is distinct from the weakest link theory. The Weibull distribution given in Section III-5 HHA for modeling the probability of

failure (POF) of graphite material, is commonly applied to other brittle materials as well. This POF calculation is made even more complex by the large variability in graphite strength, the anticipated degradation of the nuclear components during operation, and the operational-induced changes to the inherent material properties as a result of neutron irradiation and high temperatures.

Finally, there are actually several different nuclear graphite grades—each with different material properties—which can be used for nuclear applications. Their unique material property values must be considered to determine an accurate POF for each graphite component. Thus, to determine POF, the BPVC rules define a methodology based on the Weibull analysis rather than establishing a strict (deterministic) stress threshold below which a component will safely operate without threat of failure. These probabilistic-based code rules are contained in Article HHA-3000 and are used to determine POF of components that can be fabricated from a wide variety of graphite grades.

3. WEIBULL DISTRIBUTION

3.1 Description

Rather than having a fixed stress at failure in a deterministic sense, statistics uses probability theory to account for the uncertainty in the stress at failure as a stochastic process. This is accomplished using a probability density function (PDF), which relates a continuous random variable (in this case, stress at failure) to a specific probability. Letting x be a random variable with domain D , $f(x)$ is a PDF if and only if:

$$f(x) \geq 0 \text{ for all } x \in D$$

$$F(x) = \int_D f(x) dx = 1 [1]$$

Definition 1. Definition of a probability density function (PDF).

That is, a function is a PDF if and only if it produces a positive POF at all values in the domain, and if the total area under the density function curve equals 1. The Weibull distribution was published by Waldo Weibull in his 1939 paper [2]. He developed this theory because it worked well when modeling component reliability and time-to-failure events, not because it necessarily had theoretical meanings. The Weibull distribution has been used in various fields (e.g., aerospace, ceramics, and brittle materials), including for applications in areas such as dentistry and the wind industry. It is flexible, can resemble a highly skewed distribution such as the exponential, or can resemble a normal distribution.

The Weibull distribution is a PDF and has two parameterizations: the two- and three- parameter Weibull distributions. The PDF of a two-parameter Weibull distribution includes the shape and scale parameters. The shape parameter (i.e., modulus) is also called the slope, since it is the slope of the probability plot when the y-axis is transformed as: $\ln[\ln(\frac{1}{1-F(x)})]$. The slope parameter affects the failure rate, such that if the slope is less than one, the failure rate decreases monotonically; if the failure rate is greater than one, the failure rate increases monotonically. Figure 1 is a plot showing how the shape parameter affects the shape of the Weibull distribution for a fixed scale parameter and a 0 threshold parameter (discussed shortly).

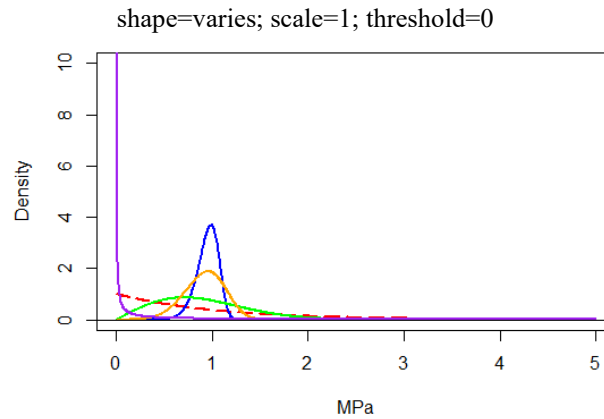


Figure 1. Weibull distribution: fixed scale and threshold, varying shape parameter.

The scale parameter stretches and shrinks the Weibull distribution as well as shifts the distribution, when the shape parameter is fixed. Figure 2 shows how the scale parameter changes the scale of the Weibull distribution for a fixed shape parameter and 0 threshold.

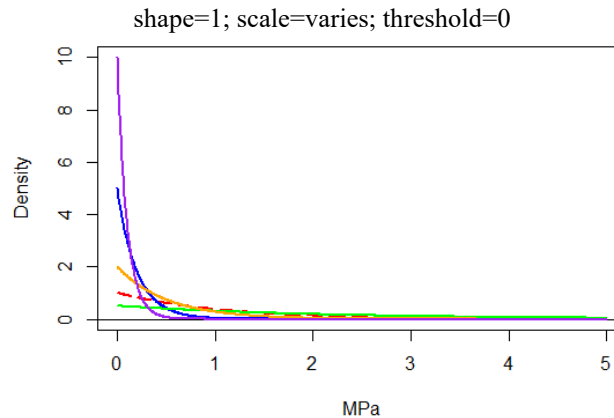


Figure 2. Weibull distribution: fixed shape and threshold, varying scale parameter.

In addition to the two aforementioned parameters, the three-parameter Weibull distribution also includes the threshold (i.e., location parameter). This parameter shifts the distribution and must be smaller than the minimum observed data point. The threshold is applied in cases where minimum times/stresses until failure exist, and this parameter is synonymous with a minimum strength. For example, Quinn and Quinn [3] states that a threshold parameter may make sense for material that has been “inspected to limit flaws over a certain size” or a “physical limit to a crack size.” Quinn and Quinn [3] also highlights the importance of carefully screening specimens via non-destructive evaluation when verifying the existence of a threshold for a given material. The two-parameter Weibull distribution is equivalent to a three-parameter Weibull distribution whose threshold parameter is set to zero. Figure 3 shows how the threshold parameter shifts the Weibull distribution to the right, for fixed scale and shape parameters.

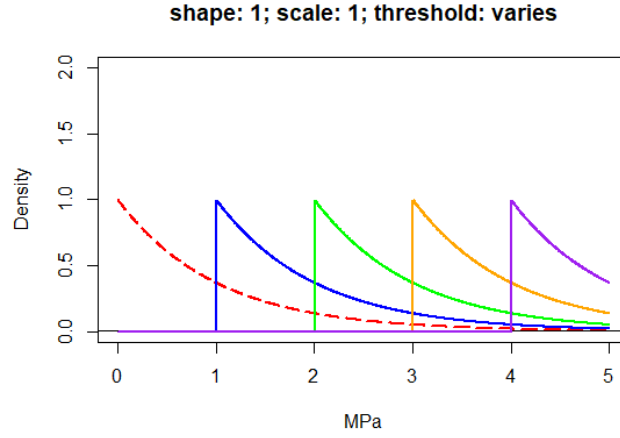


Figure 3. Weibull distribution: fixed shape and scale, varying threshold parameter.

The Weibull parameters are defined as follows:

α : shape

β : scale

θ : threshold.

Thus, the three-parameter Weibull distribution can be written as:

$$f(x) = \frac{\alpha}{\beta} \left(\frac{x-\theta}{\beta} \right)^{\alpha-1} \exp \left(- \left(\frac{x-\theta}{\beta} \right)^{\alpha} \right); 0 \text{ otherwise; where } x \geq \theta, \theta \geq 0, \alpha > 0, \beta > 0$$

Definition 2. Definition of a three-parameter Weibull distribution.

The two-parameter distribution is obtained by setting $\theta = 0$. If x is the observed stress, then $(x - \theta)$ is the observed stress minus the threshold, making it easy to see how introducing the threshold shifts the observed stresses by the threshold value. The cumulative distribution function (CDF) is defined as the cumulative POF up to a point x_0 for a Weibull distribution. Formally, the CDF of the three-parameter Weibull distribution is given as:

Equation 1. Cumulative distribution function (CDF) of the three-parameter Weibull distribution.

$$F(x) = \int_0^x f(x) dx = 1 - \exp \left(- \left(\frac{x_0 - \theta}{\beta} \right)^{\alpha} \right) \quad (1)$$

Some summary measures of a random variable that follows a Weibull distribution are:

Equation 2. Mean of three-parameter Weibull distribution.

$$\text{Mean: } E[x] = \theta + \alpha \Gamma \left(1 + \frac{1}{\beta} \right) \quad (2)$$

Equation 3. Variance of three-parameter Weibull distribution.

$$\text{Variance: } \text{Var}[x] = \alpha^2 \Gamma\left(1 + \frac{2}{\beta}\right) - E[x]^2 \quad (3)$$

where Γ is the gamma function and $\Gamma(N) = (N - 1)!$. The Weibull distribution is related to two other PDFs as:

- When the shape parameter equals one ($\alpha = 1$), the Weibull distribution is equivalent to the exponential distribution with a rate parameter equal to the inverse of the scale parameter ($\lambda = \frac{1}{\beta}$). The exponential distribution is also a common PDF in reliability statistics. It can be used to model the length of time between events in the Poisson process, such as time until failure of a component or the wait time between component failures.
- When the shape parameter equals two ($\alpha = 2$), the Weibull distribution is equivalent to the Rayleigh distribution, which is “the radial error when the x and y coordinate errors are independent normal with zero mean and the same standard deviation” [4].

The characteristic stress is a unique parameter to the Weibull distribution that gives the 63.2 percentile. It is especially useful for the 3-parameter Weibull distribution because it is the 63.2th percentile, regardless of the threshold. This characteristic stress, denoted by S_c in HHA-3217 (Calculation of Probability of Failure), is defined as $1 - \exp(-1) = 0.632$. Therefore, whenever the exponent portion of Weibull CDF is equal to one, it is the 63.2th percentile. That is, if $\frac{S_c - \theta}{\beta} = 1$, then S_c is the characteristic stress. The S_c that always makes this statement true is when $S_c = \beta + \theta$, S_c is the characteristic stress, regardless of β and θ .

The characteristic stress is the same, regardless of the Weibull parameterization. Letting there be two parameterizations of the Weibull distribution characterized by the parameters: $\alpha_1, \beta_1, \theta_1$ and $\alpha_2, \beta_2, \theta_2$. In this case, the characteristic stress of the first Weibull distribution is $S_c = \beta_1 + \theta_1$ and the characteristic stress of the second Weibull distribution is $S_c = \beta_2 + \theta_2$. Setting the two equal results in a unique property:

Equation 4. Mathematical relationship between scale parameters associated with two different threshold values.

$$\beta_1 + \theta_1 = \beta_2 + \theta_2 \rightarrow \beta_2 = \beta_1 + (\theta_1 - \theta_2) \quad (4)$$

That is, the scale parameter for a second parameterization based on a new threshold value can be obtained by adding the difference in the change in thresholds to the original scale parameter. The usefulness of this property regarding HHA-3217 is that an updated scale parameter can be obtained with just the change in threshold parameters and the original scale parameter. This derivation is shown in the update step later in this paper.

So far, the Weibull parameters have been discussed independently. However, the scale parameter depends on the shape parameter and both the shape and scale parameters depend on the threshold parameter. This will be discussed in the estimation methods section coming up next.

3.2 Weakest Link Theory

A chain of links of equally sized links can be used to understand the weakest link theory. The chain can be pulled on both ends with equal force. Once one link breaks in the chain, the entire chain is “broken”. The first link that breaks is considered the weakest link that caused the entire chain to break. The link may have broken because of a defect, such as inconsistent material thickness or a large flaw, that caused the break. The parallel analogy to graphite is: consider laying a 3D mesh over a graphite block and breaking the block into pieces of equal volume pieces. These pieces correspond to the equally sized links in the chain. The cracks and pores in the graphite volumes will govern its strength. The assumption is that whichever graphite element volume breaks first results in the failure of the entire component.

3.3 Parameter Estimation

The ASME code rules and ASTM standards specify different methods for obtaining Weibull parameter estimates. Different parameter estimation methods produce estimators with different properties. The method for obtaining parameter estimates affects the method for obtaining lower bounds. Specifically of concern is whether the estimation method affects the qualification of a component, specifically with the introduction of the threshold parameter in the full assessment.

3.3.1 Maximum Likelihood Estimation

3.3.1.1 Two-Parameter Case

For the sake of simplicity, the two-parameter Weibull distribution can be considered synonymous with the simplified assessment while the three-parameter Weibull distribution is synonymous with the full assessment, though ASTM does not use such terminology. That terminology is unique to ASME.

ASTM D-7846 [5] details the use of maximum likelihood estimation (MLE) to obtain the two-parameter Weibull distribution parameter estimates, while acknowledging that other estimation methods also exist. MLE is a common choice of parameter estimation because it provides asymptotically unbiased estimates with the minimum variance of all possible estimators. MLEs are determined by first finding the log-likelihood of the PDF, which is equal to the log of the product of the PDF evaluated at all observed data points (x_i). The partial derivatives are solved for each parameter, then set to zero. For the simplified assessment, the Weibull MLE equations for the shape and scale parameters are:

Equation 5. Maximum likelihood equation (MLE) for the shape parameter, two-parameter Weibull distribution.

$$\text{Shape: } \left[\frac{\sum_{i=1}^n x_i^\alpha \ln(x_i)}{\ln(x_i^\alpha)} - \frac{1}{\alpha} \right] = \frac{1}{n} \sum_{i=1}^n \ln(x_i) \quad (5)$$

Equation 6. Maximum likelihood equation (MLE) for the scale parameter, two-parameter Weibull distribution.

$$\text{Scale: } \hat{\beta} = \frac{\sum_{i=1}^n x_i^\alpha}{n} \quad (6)$$

The equations are solved for iteratively by using an optimization function. The scale parameter depends on the shape parameter, thus the two are not independent. Note that this provides a biased estimate of the shape parameter. (See ASTM D-7846 [5] for details on the unbiasing factor.)

ASTM D-7846 [5] utilizes pivotal quantities for MLEs in order to obtain the confidence bounds derived from Thoman et al. [6] for sample sizes of up to 120 and numerically fitted equations expanded beyond 120 samples.

3.3.1.2 Three-Parameter Case

The full assessment outlined in the ASME code includes section HHA-II-3200 [Material Reliability Curve Parameters (Three Parameter for Full Assessment)], which is used to find the Weibull parameters discussed in HHA-3217 using MLE. However, there are several reasons to avoid using the MLE in the three-parameter case. The three-parameter MLE equations are obtained via the same method used for the two-parameter MLE equations, by use of the log-likelihood. The equations are as follows:

Equation 7. Maximum likelihood equation (MLE) for the shape parameter, three-parameter Weibull distribution.

$$\text{Shape: } \hat{\alpha} = \left[\frac{\sum_{i=1}^n (x_i - \hat{\theta})^{\hat{\alpha}} \ln(x_i - \hat{\theta})}{\sum_{i=1}^n (x_i - \hat{\theta})^{\hat{\alpha}} - \frac{1}{n} \ln(x_i - \hat{\theta})} \right]^{-1} \quad (7)$$

Equation 8. Maximum likelihood equation (MLE) for the scale parameter, three-parameter Weibull distribution.

$$\text{Scale: } \hat{\beta} = \left[\frac{1}{n} \sum_{i=1}^n (x_i - \hat{\theta})^{\hat{\alpha}} \right]^{\frac{1}{\hat{\alpha}}} \quad (8)$$

Equation 9. Maximum likelihood equation (MLE) for the threshold parameter, three-parameter Weibull distribution.

$$\text{Threshold: } (\hat{\alpha} - 1) \sum_{i=1}^n (x_i - \hat{\theta})^{-1} = \frac{\hat{\alpha}}{\hat{\beta}^{\hat{\alpha}}} \sum_{i=1}^n (x_i - \hat{\theta})^{\hat{\alpha}-1} \quad (9)$$

Evans *et al.* [7] states that “computer routines to produce 3-parameter Weibull estimates often show inconsistent convergence. Numerical problems exist, which can make difficult the direct calculation of MLE using optimization routines that maximize the likelihood. When the shape parameter is less than or equal to two, the information matrix of the Weibull distribution has singularities, which means an iterative method that uses second derivatives is likely unstable”.

For this study, two functions were found in R [8] (a statistical program) that fit the three-parameter Weibull distribution using a pseudo-maximum likelihood method (pseudo-MLE). One method is the maximization of the log-likelihood function of the two-parameter Weibull distribution after considering the observed data minus the threshold (blue vertical line in Figure 4). The other R pseudo-MLE method used is to first find the threshold value that maximizes the correlation function of the linearized Weibull CDF, then use the two-parameter log-likelihood function to maximize and obtain the shape/scale parameters (red vertical line in Figure 4).

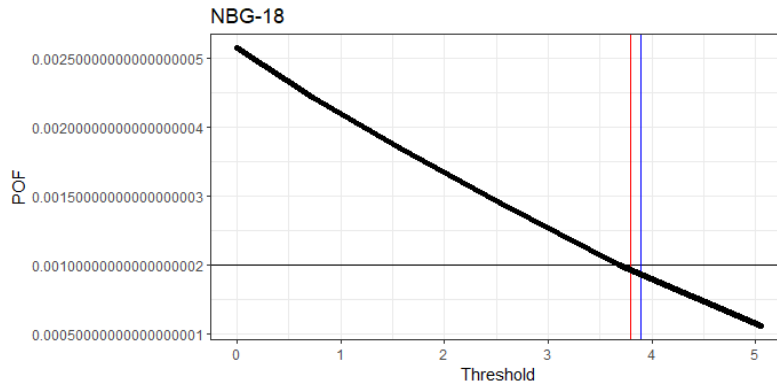


Figure 4. POF as a function of threshold: NBG-18.

NBG-18 is the only graphite grade for which the estimated threshold parameter from the pseudo-MLE methods was in a range that enabled a POF to be calculated using the fine-mesh component data. Different FEA models need to be run with loads resulting in stress distributions that make sense for the other graphite grades before a similar comparison can be done for them. For NBG-18, both methods led to similar threshold estimations; however, the difference is close to the decision point, emphasizing the importance of code rules being specific on which estimation method should be used. Because MLE of the 3-parameter Weibull distribution produces unstable estimates, when they can be found at all, and because this work indicates that the user's choice of pseudo-MLE method may affect the acceptance of a component, it is recommended the parameter estimation method is tuned with experimental results. This is discussed towards the end of the document in the proposed future validation study.

3.3.2 Least Squares Estimators

HHA-II-3100 [Material Reliability Curve Parameters (Two-Parameter for Simplified Assessment)] requires use of the linearized likelihood function that was solved for the shape and scale parameters via the least squares estimation method. The survival function is given by:

Equation 10. Survival function, two-parameter Weibull distribution.

$$L(x) = 1 - F(x) = \exp \left[- \left(\frac{x}{\beta} \right)^\alpha \right] \quad (10)$$

Using the linearization function from above:

Equation 11. Linearized version of the survival function, two-parameter Weibull distribution.

$$\ln[-\ln(L(x))] = \alpha \ln(x) - \alpha \ln(\beta) \quad (11)$$

The least squares method is then used to find the α and β parameters that minimize the squared errors.

HHA-II-3100 outlines the same method for obtaining the lower bounds as that described in ASTM-D7836 [5] for the simplified assessment. Although least squares is not commonly applied to the three-parameter Weibull distribution, it has been studied.

3.3.3 Method of Moment Estimators

Method of moment (MOM) estimators are found by setting the number of moments equal to the number of unknown parameters and then solving. Generalizing to the three-parameter case, the first three moments are obtained. The k^{th} moment is defined as $M_k = \int x^k f(x) dx$, noting that the first moment is the mean and the second is the central variance (i.e., the mean squared-error). A general overview of moment estimation can be found in Casella and Berger [1].

3.3.4 Other Considerations

Ideally, the chosen estimation method will produce parameter estimates with certain desirable properties (e.g., unbiasedness, unique and minimum variance), at least asymptotically. As will be discussed later, the major issues with Weibull parameter estimates comes with the introduction of the third parameter, the threshold. Methods for obtaining confidence intervals on Weibull parameters have not been discussed here.

3.4 Basis for Use of Weibull Distribution

Hindley [9] conducted a comprehensive review, finding that the Weibull distribution does not fit well to nuclear graphite test data.

Hindley did his own analysis by collecting tensile, flexural and compressive stress test data. He compared the fit between the normal distribution and the two-parameter Weibull distribution (Weibull-2). He found that the normal distribution did not model either tail of the stress distribution well. The Weibull2 distribution fit well in the right tail of the distribution, but the fit varied by stress test in the left tail of the distribution.

The Anderson-Darling (A-D) test suggested a poor fit for the flexural and compressive stress data ($\alpha = 0.05$). In all cases, the fit estimated a POF that was less conservative than what the data showed. Some sources suggest a bimodal distribution exists for compressive stress. As a side note, Hindley also normalized the three data sets and fit a new Weibull distribution. He showed that all three data sets conformed to the combined data set, suggesting the stress distribution is characterized by the flaw distribution inherent in the graphite, not in the specific test. This means that the test determines the mean stress at failure, while the stress distribution (variability, shape) remains similar regardless of test.

4. SIMPLIFIED ASSESSMENT

4.1 Method

ASME has code sections detailing the simplified assessment for approving graphite components. The outcome of the simplified assessment is an allowable stress. The calculated peak equivalent stress determined from the FEA modeling is compared against the allowable stress determined using the probability of failure (POF) for the component's structural reliability class (SRC). The component is accepted or rejected for the given component SRC based on whether the calculated allowable stress is below the limit. ASTM D-7846 [5] provides a more detailed explanation of the application of the Weibull distribution. There is not a minimum required number of test specimens. Steps in the ASTM for determining statistical parameters useful in the simplified assessment are:

- Censor and document outlying observations
- Obtain the 2-parameter Weibull shape and scale parameters using MLE
- Assess the goodness of fit (GOF) by using order statistics to the Weibull fit relative to the observed data
- Obtain lower bounds of 90% two-sided confidence intervals for the shape/scale parameters
- Obtain the unbiasing factor for the Weibull shape parameter
- Include the following information in a test report: material type, test procedure, number of failed specimens, failure load, stress calculation method, MLEs, unbiasing factors, details of 90% confidence interval calculations, test data reported in ascending order, mean.

ASTM provides background information on how to obtain the Weibull parameters and lower bounds in the simplified assessment that is described in ASME-3300 (Requirements for design of the Graphite Core Assembly). In ASME-II-3300 (Design Allowable Stress Value), the lower bounds obtained in Step 3 are used to find an allowable stress by inverting the CDF for a given SRC's limiting POF. Condensed equivalents to the steps described in ASTM-D-7846 are outlined in ASME-II-3100 [Material Reliability Curve Parameters (Two Parameter for Simplified Assessment)], in less detail. One notable difference is the estimation method. As previously mentioned, ASME requires the method of least squares from the linearized survival function to obtain shape/scale parameter estimates (vs. MLE in ASTM for the simplified assessment). The same method for obtaining Weibull lower bounds is utilized.

Most recently, both code sections addressing the 2-parameter Weibull distribution have been revised by aligning notation, fixing equations and adding in fitted equations which allow for parameter lower bound calculations when sample sizes are greater than 120 (developed by Heo et al. in [11]).

4.2 2020 Workshop

A virtual workshop was held by INL in 2020 to discuss several issues found in the review of the simplified assessment and to decide on how to move forward. The issues were: (1) inability to define a quantifiable amount of conservatism in the allowable stresses (thus far) (2) the dependence of the Weibull parameters and (3) the goodness of fit (GoF). Consider the definition of “confidence interval” when trying to reason what is meant by “quantifiable amount of conservatism”. The process of creating, say a 95% confidence interval, provides a quantifiable amount of conservatism on the Weibull parameter lower bounds. A 95% confidence interval on the scale parameter can be understood as an interval representing the expected sampling variability on a Weibull scale parameter, when a large number of samples of size “n” are drawn from a population. Currently, there is not a way to quantify nor understand (interpret) the amount of conservatism represented in the allowable stress as calculated currently as per the simplified assessment in ASME.

The main issue discussed was the fact that while the allowable stress is calculated using the lower 95% one-sided confidence bounds of the Weibull shape/scale parameter estimates, this does not correspond to a result that is the lower bound of a 95% one-sided confidence interval on the allowable stress. The question then posed is, how conservative is the allowable stress?

To illustrate how the current ASME method of obtaining a distribution based on lower confidence bounds on parameters, we show fitted distributions to a set of 253 dog bone tensile test specimens of NBG-18. The two-parameter Weibull MLE fit (black curve in Figure 5) fits the histogram of the observed data. The blue curve is the Weibull distribution, characterized by the lower bounds of the shape/scale parameters.

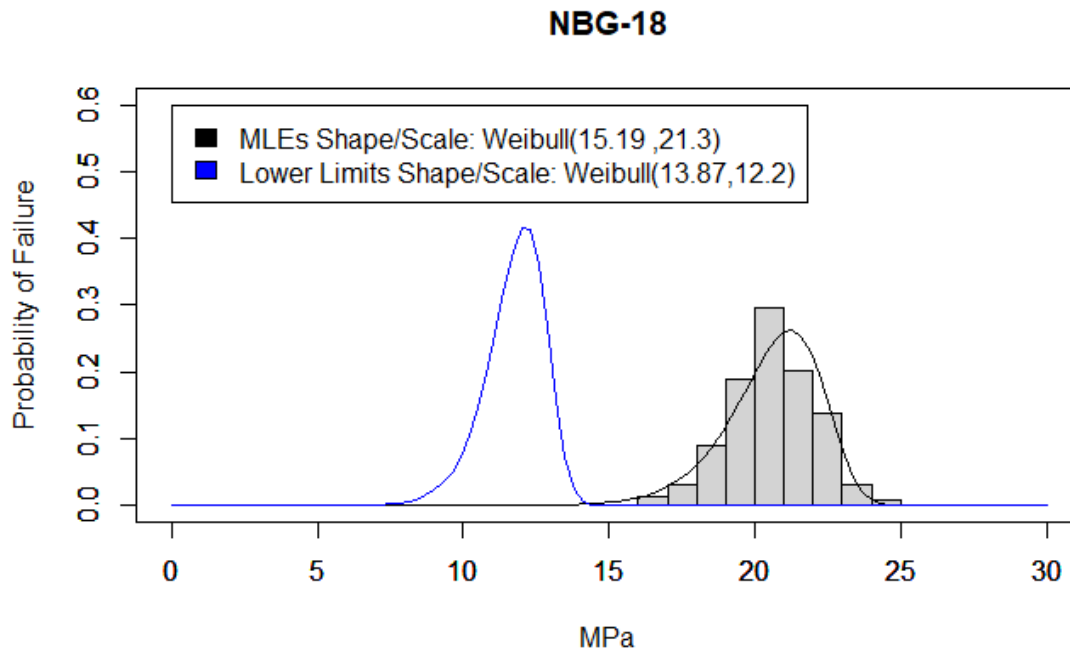


Figure 5. Comparison of MLE and lower bound distribution fits for NBG-18.

The Weibull distribution characterized by the lower bounds of the shape/scale parameter (blue curve in Figure 5) is shifted to the left of the histogram, without overlap. While the lower bound distribution calculated in this manner provides a conservative POF, it appears to be excessive. Zooming in to the stresses near the SRC-1 POF limit, we see that the lower bound distribution almost cuts the allowable stress in half relative to the MLE distribution (Figure 6).

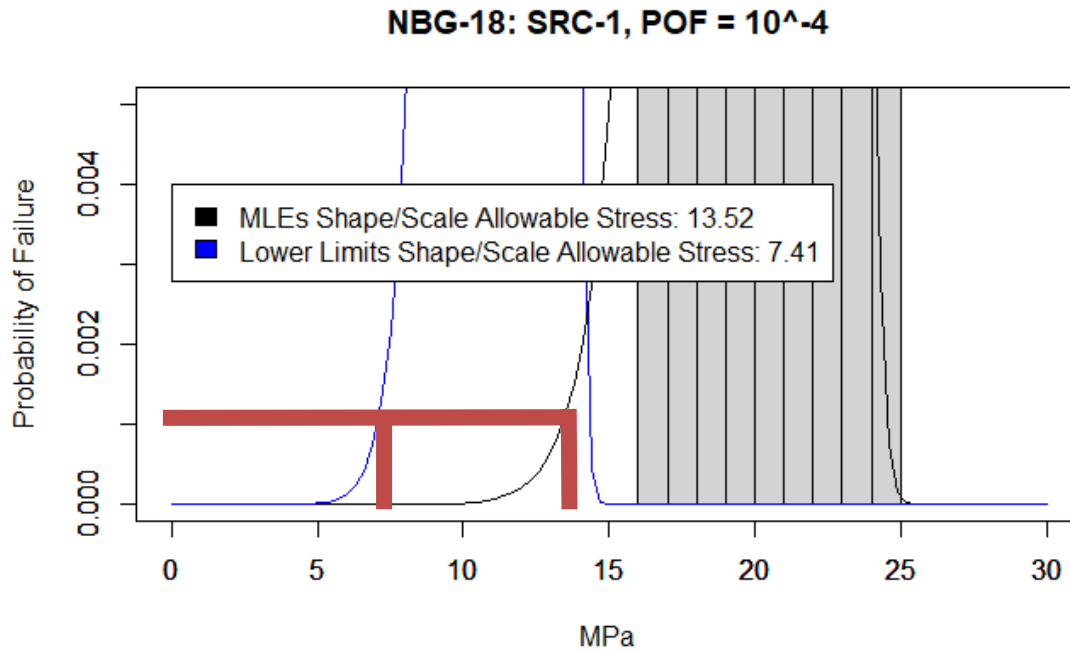


Figure 6. Comparison of POF from MLE and lower bound distribution based on SRC-1 limit for NBG 18.

Since the conservatism in the confidence interval process does not translate to the same conservatism in the allowable stress, the area of overlap was considered as a potential measure for the amount of conservatism in the lower bound distribution. The percent area of overlap between the lower bound and MLE distributions was found to be 0.238% (

NBG-18

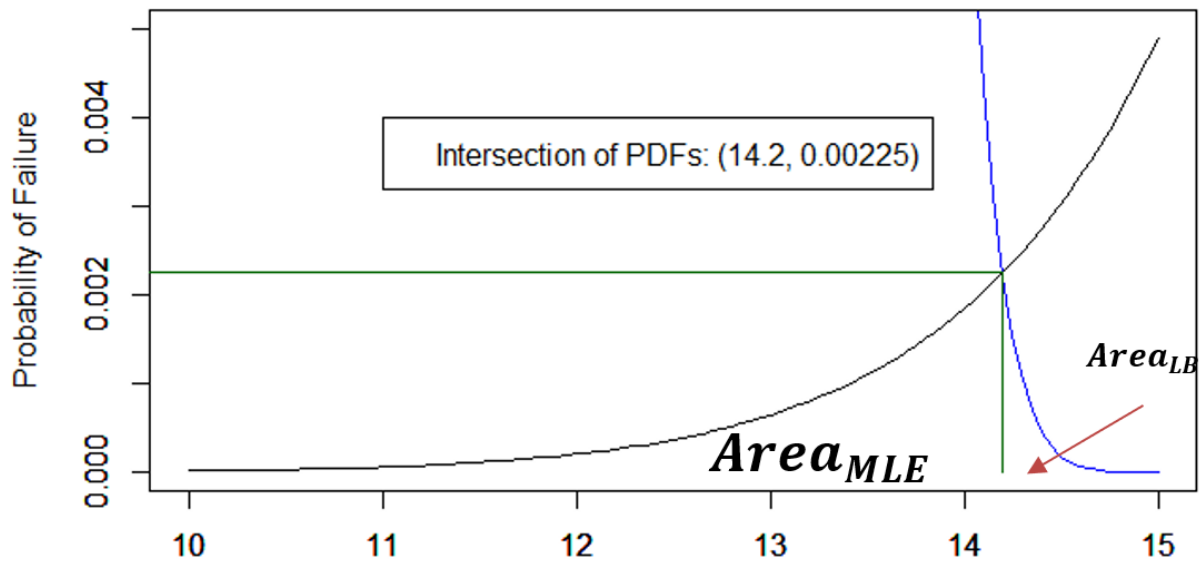


Figure 7). It was concluded that while the allowable stress calculated based on the simplified assessment appears to be conservative, a method for quantifying the amount of conservatism in the value or in the process has yet to be defined.

NBG-18

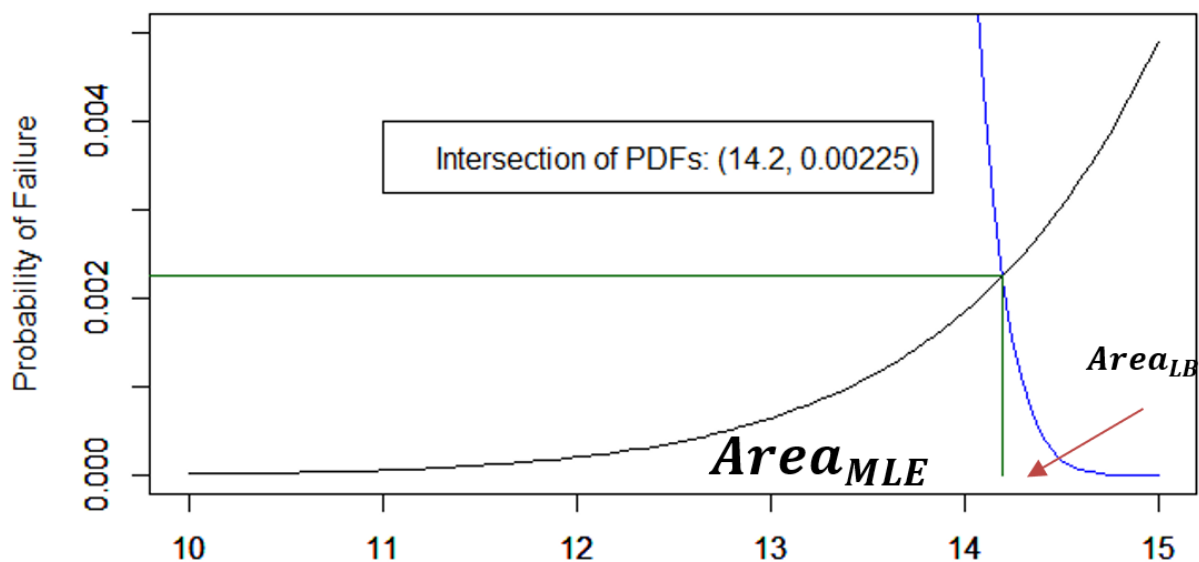


Figure 7. Zoomed in image of area of overlap for MLE and lower bound NBG-18 distributions.

In estimating Weibull parameters, Duffy and Parikha [10] used confidence rings to obtain the lower bound distribution that estimates the Weibull MLE's in a way that accounts for parameter dependence when obtaining lower bounds. The result is that the lower bound distribution resembles the shape of the MLE distribution, only shifted to the left. Practically, it makes sense that the conservative strength distribution contains a set of parameters that could reasonably be considered to have produced the observed measurements. This type of conservative strength distribution is quite different from the blue distribution in Figure 7, for which the probability of having drawn the observed data set would be very small based on the amount of overlap in the distributions.

Even if the confidence-ring-based lower bound distribution is used to obtain the allowable stress, using the 95% one-sided lower bounds on the Weibull parameters does not translate to a 95% lower bound on the allowable stress. The question still remains as to how to quantify the amount of conservatism in the allowable stress.

A different method for calculating a lower bound on the allowable stress by using the MLE distribution, and then obtaining a lower bounds on the allowable stress using statistical theory developed for obtaining bounds on quantiles of the Weibull distribution in Heo *et al.* [11] and Meeker *et al.* [12]. For NBG-18 and considering a component of SRC-1, a two-sided 90% confidence interval of (16.87, 17.59) was found around the stress of 17.23 (the 0.039th quantile, chosen arbitrarily). Figure 8 shows a plot illustrating how the quantile-quantile (Q-Q) method proposed in [11] (dashed lines) compares to the method currently used in the code to obtain a conservative allowable stress (blue).

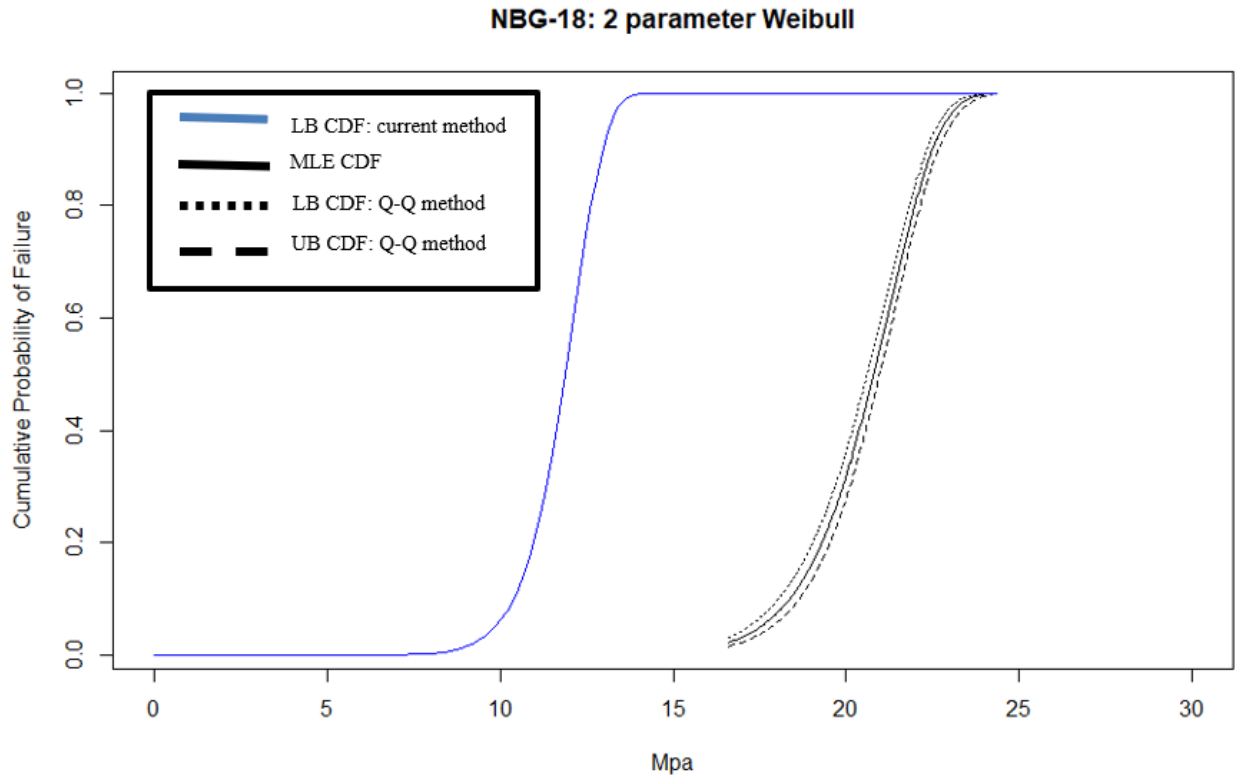


Figure 8. Comparison of lower bound Weibull CDFs.

Clearly the Q-Q method provides a much less conservative lower bound distribution. Future work will compare the Q-Q method for determining lower bound distributions with the confidence ring approach proposed by Duffy and Parikha [9], as both the parameter dependence and the amount of conservatism in the lower bound distribution are questions not addressed in the code.

The consensus from the workshop participants was that the confidence ring approach should be compared in terms of conservatism to the current lower bound distribution approach in the code. While the current method appears to be conservative, the amount of conservatism seems to be on the extreme side of conservative. The participants stated that code is developed based on best-practices and past experience, not necessarily what is theoretically correct. Therefore, since the method was adapted from the long-standing German KTA codes, and it does appear to be conservative and the committee was not comfortable with the proposed Q-Q method because of how much less conservative the resulting lower bound distribution was relative to that of the current approach.

The question then arises as to how sensitive the overlapping area of the MLE and lower bound (LB) distributions are to sampling uncertainty. The amount of overlapping area and the variability in that overlap change by graphite grade. Sample size effect wanes out between $n=50$ -250, depending on graphite grade (See Figure 9 and Figure 10). The following steps were taken:

- Calculate the MLEs from the observed data (sampled specimens).
- Let n equal the number of specimens in the observed data.
- Sample n times from a Weibull distribution based on MLEs from step 1.
- Compute the MLEs from these sampled data (call these sample.MLE).
- Compute the lower bounds of the sample.MLEs (call these sample.LB).
- Calculate the overlapping area between the sample.MLE and sample.LB distributions. (This is the area of overlap between the black and blue curves.).
- Repeat steps 2–6 1000 times.

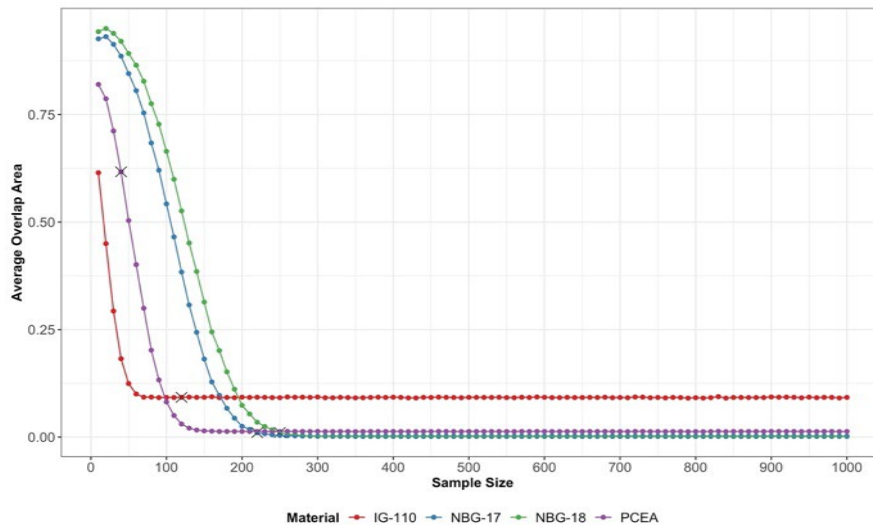


Figure 9. Average area of overlap between MLE and lower-bound distributions as a function of sample size.

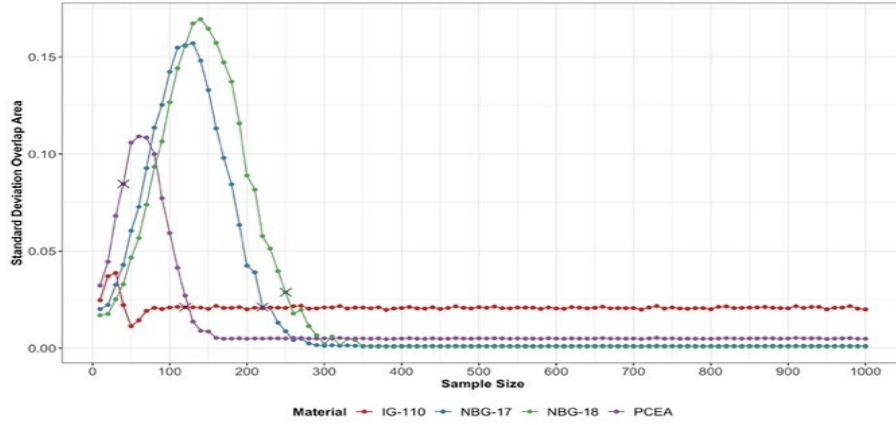


Figure 10. Variability in the area of overlap between MLE and lower-bound distributions as a function of sample size.

For reference, plots showing the MLE and lower bound distributions for NBG-17, PCEA, and IG-110 are included below in Figure 11, Figure 12, and Figure 13 for reference.

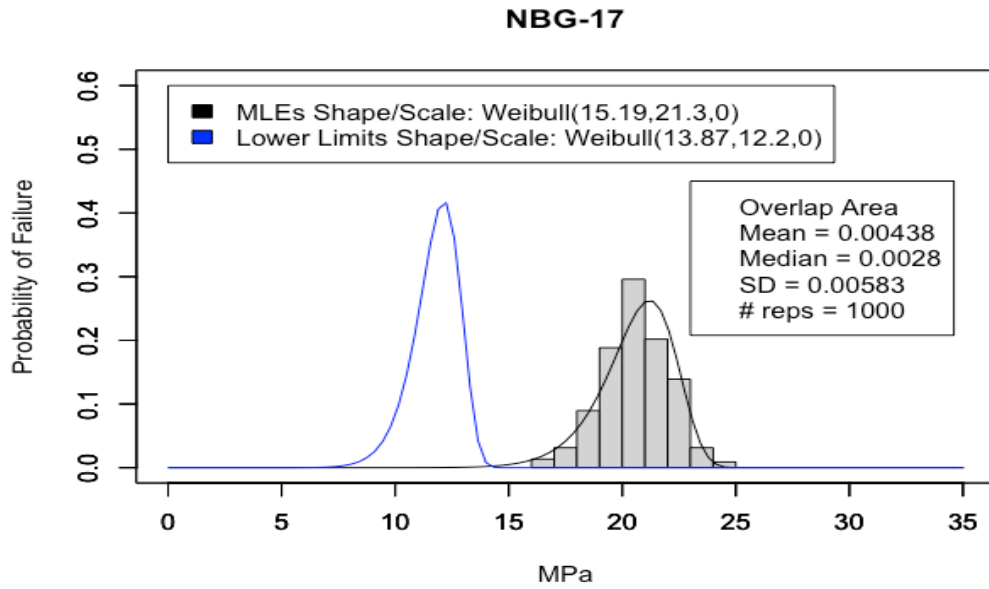


Figure 11. Comparison of MLE and lower-bound distribution fits for NBG-17.

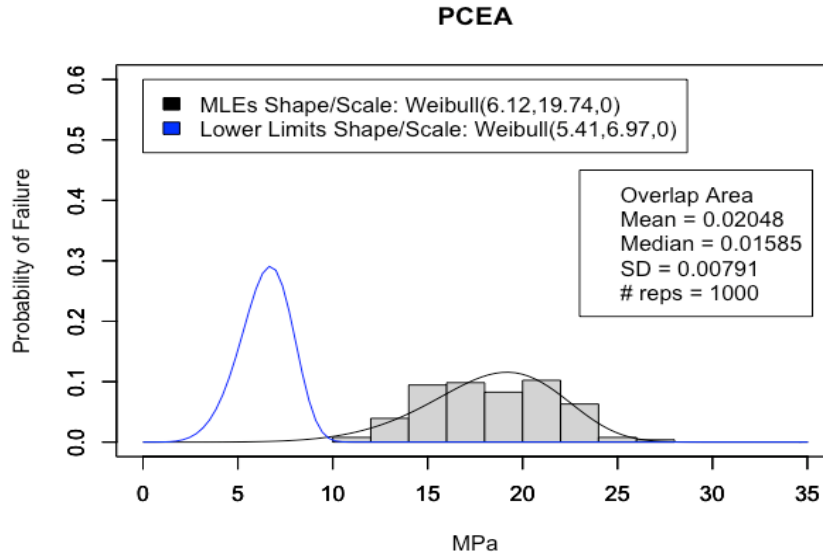


Figure 12. Comparison of MLE and lower-bound distribution fits for PCEA.

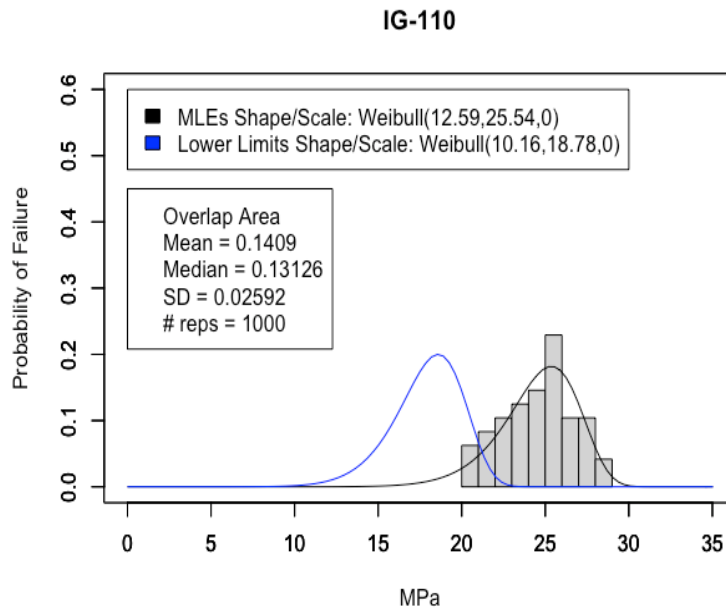


Figure 13. Comparison of MLE and lower bound-distribution fits for IG-110.

In the simplified assessment, it was concluded that sampling uncertainty exists in the allowable stress. The current method does not allow for a consistent, quantifiable amount of conservatism in the allowable stress, and it uses the lower bounds of one-sided 95% confidence intervals on the Weibull parameters as a method to implement conservatism. Note, the amount of conservatism in the Weibull parameters does not translate to the same amount of conservatism in the allowable stress. The area of overlap was used to quantify the conservatism in the MLE and lower-bound distributions. The area of overlap varied by graphite grade, causing the current method to provide an inconsistent amount of conservatism. Another

simple solution may be to just shift the MLE distribution by a certain amount. The following are two possible solutions:

- Quantile-based confidence interval on the allowable stress
 - Pro: Simple and allows for a quantifiable amount of conservatism on the allowable stress
 - Con: Less conservative than the current method.
- Distribution shift
 - Pro: Retains the shape of the data distribution
 - Con: Ad hoc method to be developed in determining the amount of shift.

Other work in this area includes confidence rings, which solve a different problem related to the dependence of the Weibull parameters. Confidence rings correctly obtain lower bounds on parameters by considering their dependence. More work is needed to understand how the confidence ring method relates to the Q-Q method, and whether it would lead to a quantifiable amount of conservatism measurable by some metric such as a consistent area of overlap between the MLE and lower-bound distributions, regardless of graphite grade. As things currently stand, however, the amount of conservatism, when measured by area of overlap, changes by graphite grade.

4.2.1 Goodness of Fit Analysis

Goodness of Fit (GoF) was evaluated for four graphite grades: NBG-18, NBG-17, PCEA, and IG-110 in Figure 14. The shape and scale parameters were found using MLE. Note that this is an evaluation of how well the MLE Weibull distribution fits the observed data, not how well the lower-bound distribution fits the data, as was the case above. This may be useful for comparing against the analysis presented in Hindley's basis work.

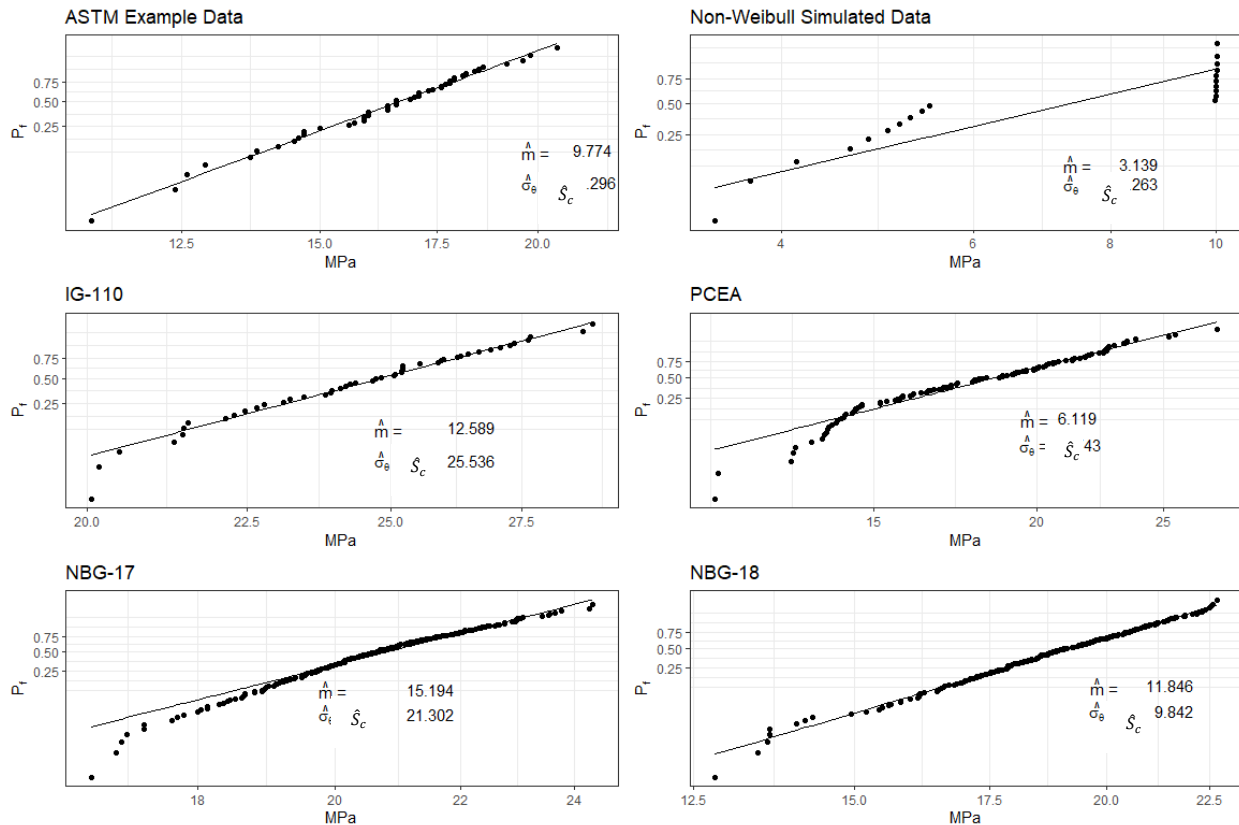


Figure 14. Goodness-of-fit plots.

The GoF tests used were: Anderson-Darling (AD), Kolmogorov-Smirnov (KS), and the Cramer-von Mises (CM). The null hypothesis of the tests was that the Weibull fit was adequate for the observed data. The alternative was that the Weibull fit was inadequate for the observed data. A p-value < 0.05 would provide strong evidence of a poor fit. The GoF test suggest a poor fit for NBG-17, PCEA, and the non-Weibull simulated data. Based on a visual inspection of Figure 14 above, the test seems to be correctly identifying deviations. Note that the poor fit occurs in the left tail of the distribution. This is of concern because the SRC POF limits are in the left tail. If the fit is poor in the left tail, added conservatism may be needed. Table 1 below summarizes the GoF test results.

Table 1. Goodness of fit statistics output.

ASTM D-7846 Example Data			
Test	Critical Value (alpha = 0.05)	Test Statistic	P-value
AD	0.757	0.1893	0.915
KS	–	0.442	0.880
CM	0.124	0.02836	0.885
Non-Weibull Simulated Example Data			
Test	Critical Value (alpha = 0.05)	Test Statistic	P-value
AD	0.757	2.646	< 0.001
KS	–	1.501	< 0.001
CM	0.124	0.454	< 0.001
IG-110			
Test	Critical Value (alpha = 0.05)	Test Statistic	P-value
AD	0.757	0.223	0.81
KS	–	0.646	0.30
CM	0.124	0.0279	0.89
PCEA			
Test	Critical Value (alpha = 0.05)	Test Statistic	P-value
AD	0.757	0.817	0.02
KS	–	0.717	0.255
CM	0.124	0.102	0.12
NBG-17			
Test	Critical Value (alpha = 0.05)	Test Statistic	P-value

AD	0.757	1.402	< 0.001
KS	–	1.041	< 0.001
CM	0.124	0.230	< 0.001
NBG-18			
Test	Critical Value (alpha = 0.05)	Test Statistic	P-value
AD	0.757	0.211	0.895
KS	–	0.540	0.665
CM	0.124	0.033	0.790

5. FULL ASSESSMENT

5.1 Method

The full assessment is outlined only in ASME. The main methodology is outlined in HHA-3217, with reference to equations found in HHA-II-3200. In this report, the notation is defined as follows:

- Shape: m
- Characteristic stress: S_c
- Threshold: S_0
- Equivalent stress: σ
- Element volume: v .

Primes indicate an updated parameter. Subscripts of 0.95 and 0.05 indicate the lower bound of a one-sided 95% confidence interval. Highlighted sections are not currently implemented in the code but are being considered as additions and will be discussed later in this report. This section is dealing with the full assessment and its use in the qualification of graphite components. The output of the full assessment is a POF, which is compared to the POF limit for the component's SRC POF limit. The full assessment requires two datasets as inputs: the material tensile test data and the component 3-D finite element analysis (FEA) equivalent stresses based on a mesh with element volumes. The steps in the full assessment are outlined below, with highlighted sections indicating revisions that are not currently in the code:

- Obtain the lower bounds of the shape ($m_{0.05}$) and scale ($S_{c0.05}$) parameters, as well as that of the associated threshold parameter (S_0), from a three-parameter Weibull fit.
- Arrange the component data in decreasing order of the equivalent stresses.
- (Update Step) Reduce the threshold if the maximum equivalent stress is less than the lower bound of the scale parameter; specify the (reduced) threshold as ($S'_0 = \frac{\sigma_{max}}{S_{c0.05}} S_0$).
- Update the shape ($m'_{0.05}$) and scale ($S'_{c0.05}$) lower bounds, using the reduced threshold S'_0 .
- Remove any component equivalent stresses less than S'_0 .
- Calculate $X_i = \left[\frac{\sigma_{vi} - S'_0}{S'_{c0.05} - S'_0} \right]^{m'_{0.05}}$.

- Group integration volumes based on:
 - Volume grouping criteria
 - Stress range criteria.
- Compute the probability of survival for each group: $L_I = \exp \left[- \left(\sum_i \sigma_{vi} * \frac{v_i}{V_I} \right) \right]$.
- Find the probability of failure: $POF = 1 - \prod_I L_I$.
- Compare the calculated POF to the allowable POF for the given SRC.

5.2 Sensitivity Analysis Results Presented at the 2022 Workshop

5.2.1 Maximum Likelihood Estimation and the Threshold Parameter

While several of the areas outlined previously have been proposed as ASME code rule changes, several more complex issues within the code remain (primarily within the full assessment code rules section). Due to the complexity of the issues and the proposed changes to the code rules a Task Group under the ASME Working Group for Nonmetallic Design and Materials has been created. This Task Group will be addressing these more complex issues both internally within the ASME community as well as holding public workshops to provide as wide a viewpoint as possible before code rule changes are suggested. The following issues will be addressed within these future workshops.

As mentioned, MLE is a general method for finding parameter estimates of PDFs. MLE provides the parameter estimate combination considered most likely given the observed material dataset. This method is effective due to the fact that MLEs are asymptotically normal, consistent, and efficient. These are statistical terms describing parameters that are asymptotically unbiased with the minimum variance of all other estimators (under certain regularity conditions, met by the Weibull PDF).

The MLE method works by first identifying the partial derivatives of the likelihood function for each parameter, then setting them to be equal to zero. The likelihood function is the joint probability of the observed dataset. It is found by taking the product of the probability of each individual data point, and is typically denoted as $L(\hat{\theta}|\mathbf{x})$, where $\hat{\theta} = \{\hat{m}, \hat{S}_c, \hat{S}_0\}$ and $\mathbf{x} = \{x_1, x_2, \dots, x_n\}$. The likelihood function is given as:

Equation 12. Likelihood function, three-parameter Weibull distribution.

$$L(\hat{\theta}|\mathbf{x}) = \prod_{i=1}^n \frac{\hat{m}}{\hat{\beta}} * \left(\frac{x_i - \hat{S}_0}{\hat{\beta}} \right)^{\hat{m}-1} e^{-\left(\frac{x_i - \hat{S}_0}{\hat{\beta}} \right)^{\hat{m}}} \quad (12)$$

The log-likelihood function is:

Equation 13. Log-likelihood function, three-parameter Weibull distribution.

$$\ln [L(\hat{\theta}|\mathbf{x})] = \sum_{i=1}^n [\ln(\hat{m}) - \hat{m} \ln(\hat{\beta}) + (\hat{m} - 1) [\ln(x_i - \hat{S}_0)] - \left(\frac{x_i - \hat{S}_0}{\hat{\beta}} \right)^{\hat{m}}] \quad (13)$$

Taking the partial derivatives with respect to each parameter and setting them to be equal to zero yields the following maximum likelihood equations, also found in HHA-II-3200:

Equation 14. Scale parameter MLE, three-parameter Weibull distribution.

$$\hat{S}_c = \left(\frac{1}{n} \sum_{i=1}^n (x_i - \hat{S}_0)^{\hat{m}} \right)^{\frac{1}{\hat{m}}} \quad (14)$$

Equation 15. Shape parameter MLE, three-parameter Weibull distribution.

$$\hat{m} = \left[\frac{\sum_{i=1}^n (x_i - \hat{S}_0)^{\hat{m}} \ln(x_i - \hat{S}_0)}{\sum_{i=1}^n (x_i - \hat{S}_0)^{\hat{m}-1} \ln(x_i - \hat{S}_0)} \right]^{-1} \quad (15)$$

Equation 16. Threshold parameter MLE, three-parameter Weibull distribution.

$$(\hat{\alpha} - 1) \sum_{i=1}^n (x_i - \hat{s}_0)^{-1} = \frac{\hat{m}}{\hat{s}_c} \sum_{i=1}^n (x_i - \hat{s}_0)^{\hat{m}-1} \quad (16)$$

These equations must be solved for simultaneously, however, that is difficult, if not impossible to do.

Found in the “weibullness” packages in the software program R [8] is a function called `weibull.mle`, which is used to fit the three-parameter Weibull distribution. Rather than solving these three equations simultaneously, `weibull.mle` first sets a threshold value that maximizes the correlation of the linearized Weibull plot, then solves the two-parameter Weibull MLE equations for the shape and scale parameters.

5.2.2 Update Step and Shape Effect

Currently, HHA-3217 explicitly provides an update step for the threshold parameter and subsequently uses the corresponding updated version of the scale parameter. Since the shape and scale parameters depend on the threshold value, it makes sense that the lower bounds of the shape and scale parameters should be updated as well. However, the code currently does not indicate that the shape parameter is updated. Use of the lower bounds of the updated shape/scale parameters has been suggested for inclusion as a revision and is highlighted in the fourth bullet above.

The effects of updating the scale and shape parameters independently were also explored. It was found that the shape parameter does not greatly affect the POF, regardless of whether using the lower bound of the shape parameter or the MLE.

The question has arisen as to why the threshold update step is needed in the first place. Consider the five distributions in Figure 15 and in Figure 16 below: the component stress distribution (black), the original pseudo-MLE distribution (blue), the updated MLE distribution (green), the lower-bound material distribution based on the original threshold value (red), and the lower-bound material distribution with the updated parameter lower bounds (orange). Zooming in (Figure 16), we see how much of the material lower-bound distributions overlap with the component distribution. This is important because all data points that fall below the threshold have a POF of zero. By reducing the threshold, more data points contribute to the POF, thus increasing its conservatism. Table 2 provides the Weibull parameters associated with the four fits to the NBG-18 data associated with Figure 15 and Figure 16.

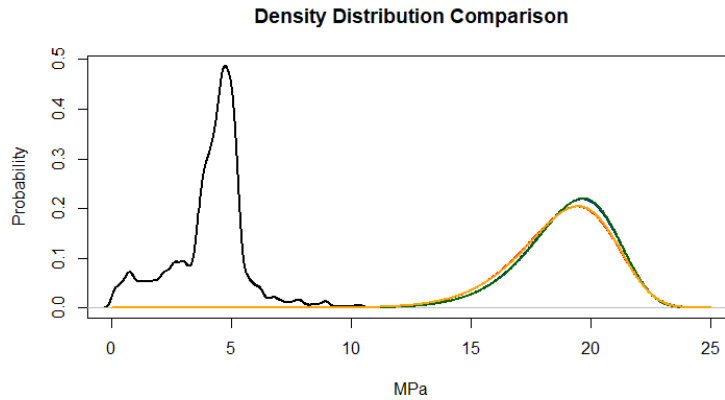


Figure 15. Five distributions used in full assessment POF calculations: NBG-18.

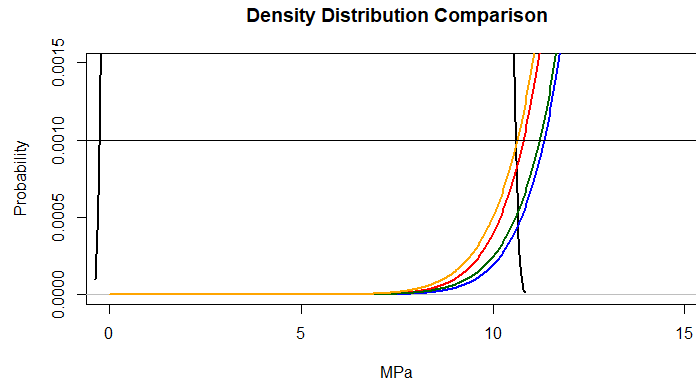


Figure 16. Five distributions used in full assessment POF calculations: NBG-18, zoomed in.

Table 2. Weibull parameters associated with Figure 15 and Figure 16.

Distribution/Parameter	Threshold	Scale	Shape
Original “pseudo-MLE”	3.8	16.0162	9.497
Original Lower Bound	3.8	15.845	8.72
Updated MLE	2.5	17.32	10.3
Updated Lower Bound	2.5	17.15	9.46

In addition to the sliding threshold’s ability to address low-probability data points, this section of Hindley’s thesis suggests that it prevents the proportion of the component volume below the threshold from being too large. Stresses below the threshold do not influence the component POF. Statistically, this always holds true, since stresses below the threshold are assigned POF = 0. However, it may not practically hold true for a graphite component if too much of the component volume is below the threshold (e.g., a low stress applied to a small portion of the component is unlikely to influence the component POF). However, if a large portion (volume) of the component is stressed below the threshold, even the low stress may influence the overall component POF. Therefore, the threshold is shifted down in certain cases to ensure avoidance of this scenario.

The previous paragraph explains why the threshold update step is needed, but it remains unclear where the method for threshold reduction originated (threshold reduction equation is $S'_0 = \frac{\sigma_{max}}{S_{c095\%}} S_0$). The update step does not guarantee that a certain percentage of the component volume will have non-zero-POF stresses (stresses above the threshold). However, it does guarantee that more component stresses will have non-zero POF than if the threshold is not reduced (thus making the calculations more conservative), and it will always reduce the threshold by the same proportion, regardless of the initial threshold value. Note, however, that the threshold reduction is not limited in the sense of there being a true threshold that is reachable by the current reduction method.

Whether the shift is justified in giving more low-probability component stresses non-zero failure probabilities, or ensuring that a large enough volume of the component exceeds the threshold, the threshold shift step seems to be something that ought not be excluded from the code. The update step also adds needed conservatism since the Weibull distribution fit is less conservative for low stresses than what is empirically observed. This is something that may not be captured when using the lower bounds.

5.3 Mesh Size Effects

HHA-3217 does not specify component mesh size requirements for the FEA. A sensitivity study was conducted to compare the effect of mesh size on POF. Three types of meshes were generated using the same stress distribution: fine, super fine, and extra super fine. The fine mesh contained 11,536 elements, the super fine mesh contained 38,934, and the extra super fine mesh contained 92,288. Obviously, in comparison with the fine mesh, the super fine mesh must contain smaller elements to cover the same component. The element volume distributions for the fine and super fine meshes are displayed below in Figure 17.

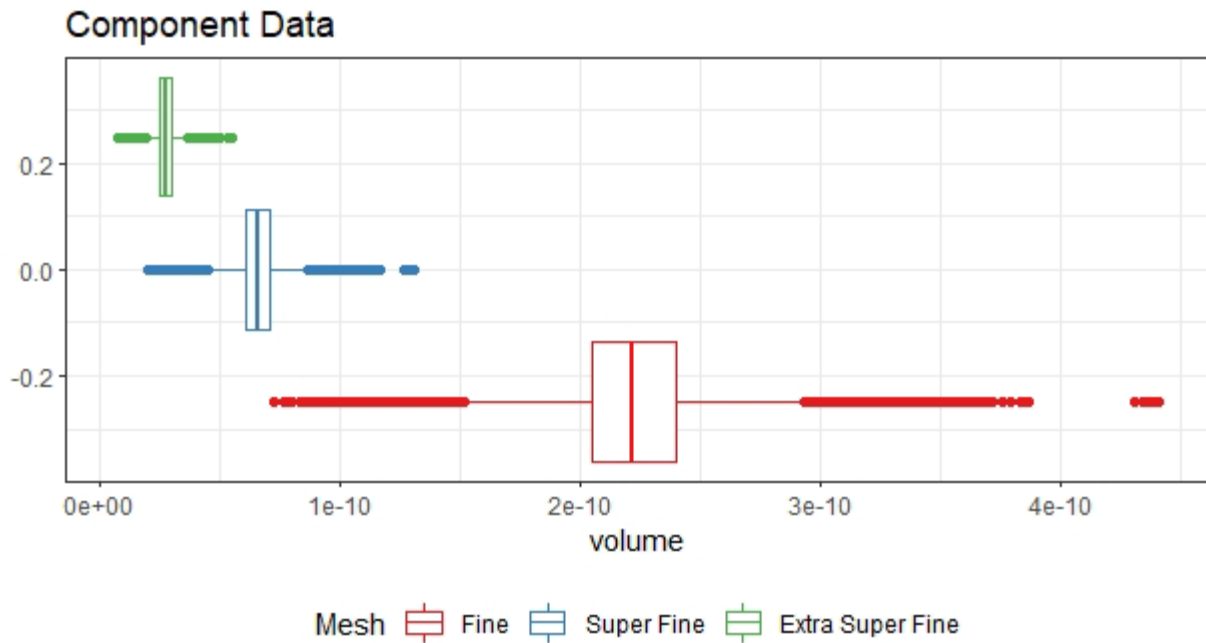


Figure 17. Component volume distributions.

The component stress distribution relative to the material strength distribution should also be considered. Note that, in this application, NBG-18 was the material used. Figure 18 shows the stress distributions to be identical for both meshes, as well as being well below the material strength distribution. This suggests that the POF for both components should be small.

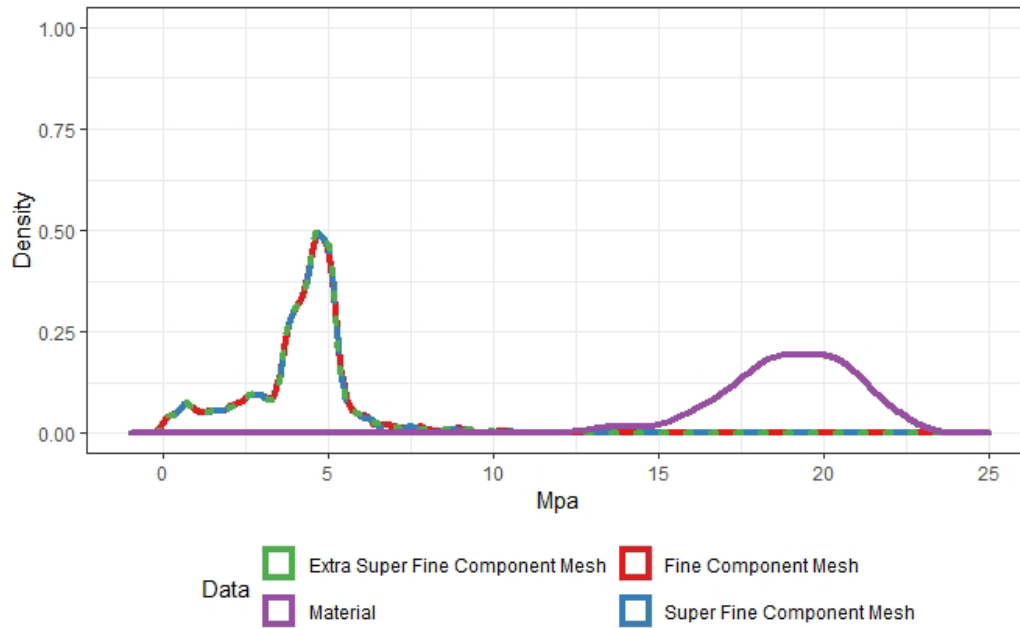


Figure 18. Component stress distributions vs. NBG-18 test data stress distribution.

The results show that mesh size affects the POF calculations, especially at low thresholds (where more component data are retained for the POF calculations). The super fine mesh gives more conservative (larger) POF. For example, SRC-1 components are required to have a POF of less than 10^{-4} . In this example, it appears there would be a discrepancy in qualification, simply due to the mesh size when the threshold is around 8.97. The extra super fine mesh has a higher POF at the same thresholds and is therefore more conservative. When the threshold is 8.97 MPa, the POF is less than 10^{-4} when using the fine and super fine meshes, and greater than 10^{-4} when using the extra super fine mesh. Figure 19 and Figure 20 illustrate how mesh size can determine whether or not the graphite component can be successfully qualified. Table 3 provides the corresponding values plotted in Figure 19 and in Figure 20.

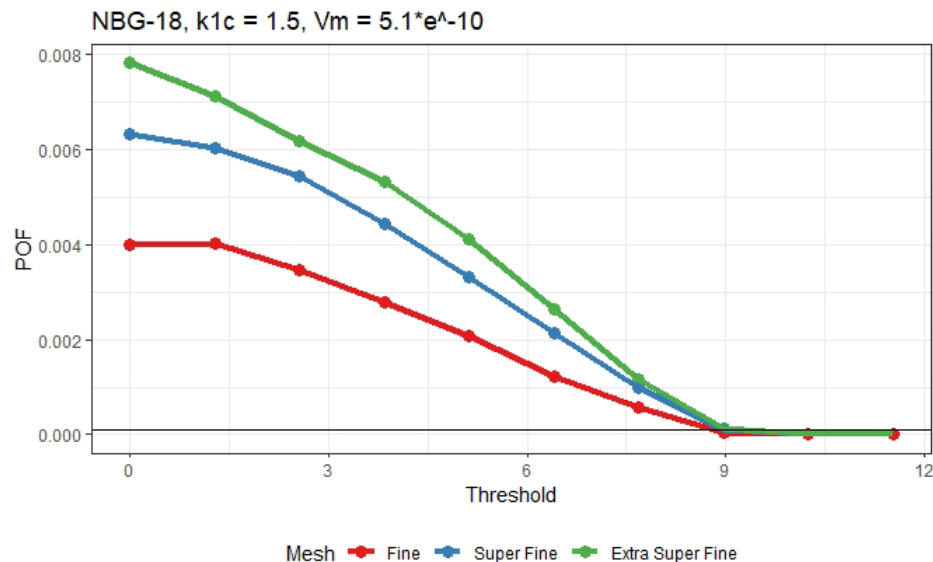


Figure 19. NBG-18: POF as a function of threshold and mesh size.

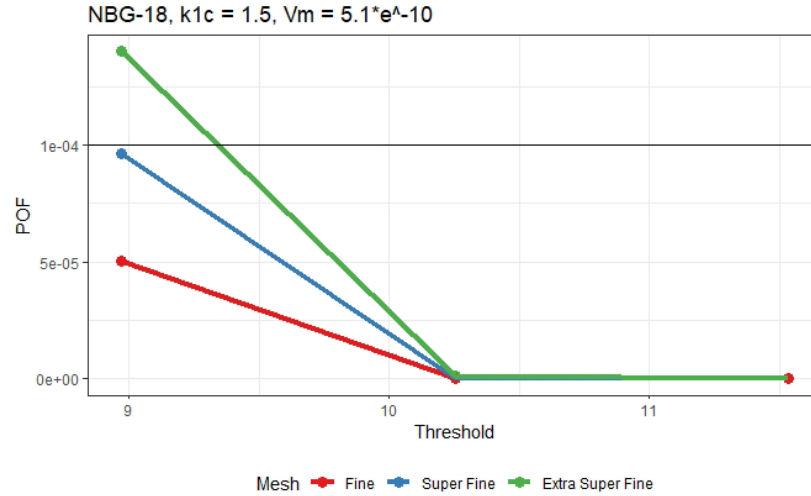


Figure 20. NBG-18: POF as a function of threshold and mesh size, zoomed in.

Table 3. Table of POF values as a function of original threshold, updated threshold and mesh size.

Mesh	Threshold/Updated Threshold	POF
Fine	0/0	4.01×10^{-3}
Super Fine	0/0	6.32×10^{-3}
Extra Super Fine	0/0	7.82×10^{-3}
Fine	1.28/0.727	4.03×10^{-3}
Super Fine	1.28/0.744	6.04×10^{-3}
Extra Super Fine	1.28/0.753	7.14×10^{-3}
Fine	2.56/1.56	3.479×10^{-3}
Super Fine	2.56/1.6	5.46×10^{-3}
Extra Super Fine	2.56/1.62	6.19×10^{-3}
Fine	3.84/2.53	2.79×10^{-3}
Super Fine	3.84/2.6	4.44×10^{-3}
Extra Super Fine	3.85/2.62	5.33×10^{-3}
Fine	5.13/3.685	2.089×10^{-3}
Super Fine	5.13/3.77	3.31×10^{-3}
Extra Super Fine	5.13/3.82	4.13×10^{-3}
Fine	6.41/5.05	1.23×10^{-3}
Super Fine	6.41/5.18	2.14×10^{-3}
Extra Super Fine	6.41/5.24	2.65×10^{-3}
Fine	7.69/6.73	5.6×10^{-4}
Super Fine	7.69/6.88	9.77×10^{-4}
Extra Super Fine	7.69/6.97	1.16×10^{-3}
Fine	8.97/8.81	5.016×10^{-5}
Super Fine	8.97/8.97	9.61×10^{-5}
Extra Super Fine	8.97/8.97	1.39×10^{-4}

Mesh	Threshold/Updated Threshold	POF
Fine	10.25/10.25	3.03×10^{-9}
Super Fine	10.25/10.25	3.61×10^{-7}
Extra Super Fine	10.25/10.25	1.22×10^{-6}
Fine	11.54/11.54	0
Super Fine	11.54/11.54	0
Extra Super Fine	11.54/11.54	0

5.4 Grouping Step

5.4.1 Weibull's Weakest Link Theory

Weibull's weakest link theory assumes that the largest flaw (crack/pore) determines the strength of the entire test specimen. It is often explained using the link chain example. If a link chain is pulled with equal force in both directions, the breaking of one link will cause the entire chain to fail. Quinn and Quinn [3] provide another example illustrating Weibull's weakest link theory by referencing da Vinci's description of sand-filled baskets suspended from wires. The baskets with shorter wires hold more sand, because shorter wires are less likely to have defects. Weibull's weakest link theory thus indicates that the larger the volume of material, the higher the POF, because larger volumes of material are more likely to contain larger flaws.

Suppose a normal flaw-size distribution in a large billet of graphite, and that the large billet is divided into 1000 smaller test specimens, which are tested for tensile strength. The largest flaw in each small test specimen determines its strength. The distribution of the largest flaws in the test specimens is assumed to be a skewed extreme value distribution (e.g., the Weibull distribution). Several types of distributions fall into this extreme value distribution category. Quin and Quin [3] state that the Weibull and Gumbel distributions have been shown to model brittle materials well, but that theory tends to align better with the Weibull distribution. As larger test specimens are taken, the strength distribution shifts left (e.g., the material becomes weaker as the flaw distribution shifts right). Typically, a few test specimens will have extremely large flaws (which break at a light load), leading to a skew in the strength distribution. This means that a different strength distribution is needed for each volume of material. If a Weibull distribution is fit based on flaws in various sized specimens, the variability in strength will stem from the variability in both the volume and the largest flaw size (as opposed to just the latter) within each specimen, and the fit may be poor.

5.4.2 Criteria

The material properties do not align with Weibull's weakest link theory. Hindley [9] cited Ho's work, which found that the strength of a test specimen "decreases as the gauge diameter of the specimen decreases below 10 times the maximum grain size". This formed the basis for the volume grouping criteria, where mesh elements are combined until the total volume exceeds 10 times the maximum grain size. As per Hindley [9]:

The methodology is based on the hypothesis that once the volume of the material being analysed reaches a certain size, the dissipation of energy between the microstructural elements is sufficient for the material to show a homogeneous macroscopic failure response. The macroscopic failure response is measured during mechanical testing of components (tensile test, bending test and compressive test). This macroscopic failure response is approximated by a weakest link failure formulation. The approximation is achieved by a volume grouping method, which defines the physical size of a link in the weakest link calculation. The term "link volume" is used to describe the volume of material considered to be necessary for NBG-18 nuclear graphite to exhibit homogeneous macroscopic failure response [78].

Hindley's Reference:

[78]: Hindley, M.P., et al., A Numerical Stress Based Approach for Predicting Failure in NBG-18 Nuclear Graphite Components with Verification Problems. Journal of Nuclear Materials, 2013. 436(1-3): p. 175-184.

It should be noted that the code rules in ASME HHA-3217 specifying the minimum link volume to be calculated using ten times the maximum grain size until the 2021 version, see Figure 21.

2019 Version:	2021 Version:
<p>(4) Group the integration volumes into groups (designated by the index I, II, III,...), starting with the point of highest stress. The allocation to groups is based on the following two conditions:</p> <ul style="list-style-type: none"> • Condition 1: group volume $V_{I, II, III, \dots} > V_m$. • Condition 2: group stress range as follows: $\frac{\max(X_{I, II, III, \dots}) - \min(X_{I, II, III, \dots})}{\min(X_{I, II, III, \dots})} \geq \Delta$ <p>where</p> <p>V_m = a process zone volume, which is the volume described by the cube of 10 times the maximum grain size</p> <p>Δ = the stress range parameter, 7%.</p>	<p>(4) Group the integration volumes into groups (designated by the index I, II, III,...), starting with the point of highest stress. The allocation to groups is based on the following two conditions:</p> <ul style="list-style-type: none"> - Condition 1: group volume $V_{I, II, III, \dots} > V_m$. - Condition 2: group stress range as follows: $\frac{\max(X_{I, II, III, \dots}) - \min(X_{I, II, III, \dots})}{\min(X_{I, II, III, \dots})} \geq \Delta$ <p>where</p> <p>V_m = a process zone volume, which is calculated from the following equation:</p> $V_m = \left[\frac{\pi}{2} \times \left(\frac{K_{IC}}{\sigma_m} \right)^2 \right]^3$ <p>Δ = the stress range parameter, 20%</p>

Figure 21. Step (4) from the 2019 and 2021 ASME BPVC versions.

The 2021 version of the code changed the process zone volume equation in order to base it on the critical stress intensity factor (K_{Ic}) instead of the maximum grain size. The formula for the process zone diameter originated from Griffith's earlier work and reproduced by [13] utilizing the concept that a material will yield at a crack tip as the stresses continue to build-up. Material yielding occurs inside a volume of inelastically deformed material along the crack front defined as the process zone, Figure 22. The size of the inelastic zone, r_{inm}^* under a monotonic tensile stress, σ_{inm}^* , is then approximated by substituting $\sigma = \sigma_{in}$ for the horizontal plane, $\theta = 0$.

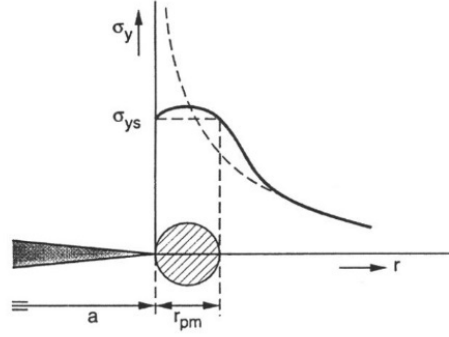


Figure 22. Schematic defining the process zone parameters.

This can be expressed as:

Equation 17. Process zone diameter equation.

$$r_{inm}^* = \frac{1}{2\pi} \left[\frac{K_I}{\sigma_{in}} \right]^2 \quad (17)$$

From which a few items can be observed:

- r_{pm} , which corresponds to r_{inm}^* in equation 17, is the process zone *diameter*, not the radius.
- From the 2021 BPVC, it can be seen that $r_c = \frac{\pi}{2} * \left(\frac{K_{Ic}}{\sigma_m} \right)^2$, which is incorrect. It is assumed that r_c was mistakenly identified as the radius of the process zone, and not as the correct interpretation as the diameter of the zone. Thus, the 2021 version of r_c is calculated to be too large by π^2 , or roughly 10 times.
- Both the 2019 and 2021 versions of the code use a cubic process zone volume which exacerbates the process zone diameter calculation mistake by three orders of magnitude (roughly 1000).

One interesting aspect of the corrected equation is that it leads to a process zone size approximately equal to 10 times the grain size for fine-grain grades (2114 and IG-110), whereas the process zone size is approximately the grain size for PCEA (800 μm), and half the grain size for NBG-18 (1600 μm).

As the V_m increases, the POF decreases. Relative to the 2019 version V_m , the corrected 2021 V_m decreased for large grain sizes, so the resulting POF will be larger and more conservative for PCEA and NBG-18. Because the corrected 2021 version always results in a smaller process zone volume size, the resulting POF calculations will always be more conservative in the corrected 2021 version than in the 2019 version of the BPVC. Note that these statements are made without considering the effect of Δ on the number of elements in each group—and therefore the resulting POF.

Table 4 below was taken from [13] with columns added to compare the corrected process zone diameter/volumes with those that would have been obtained from the 2019 version of the ASME code.

Table 4. Expanded version of Table 3 from [13].

Grade/notch orientation	Filler Particle Size (mm)	Ten. Stren. (Manufact data Mpa)	$K_{Ic} (\sqrt{m})$	r_c (mm) 2021	r_c (mm) 2021 corrected	V_m - 2021 (mm ³)	V_m 2021 corrected (mm ³)	2019 (mm ³)
2114 (WG)*	0.013	34.7	1.15	1.72	0.175	2.68	0.0028	0.0022
2114 (AG)*	0.013	34.7	1.15	1.72	0.175	2.68	0.0028	0.0022
IG-110	0.02	24.5	1.07	2.99	0.304	14.05	0.0147	0.0080
PCEA (WG)	0.8	16	1.33	10.85	1.1	668.14	0.70	512
PCEA (AG)	0.8	20	1.48	8.6	0.872	332.56	0.35	512
NBG-18 (WG)**	1.6	21	1.36	6.58	0.668	149.42	0.16	4096
NBG-18 (AG)**	1.6	20	1.41	7.8	0.791	248.66	0.26	4096

Relative to the total volume, the V_m is relatively identical when comparing the 2019 and 2021 code versions for the larger grain grades: PCEA and NBG-18. The change was made specifically to increase the V_m for the finer grades, which we see that the 2021 implementation does by at least 1000 times. This was deemed necessary because the POF calculations were overly conservative. For example, with IG-110 the cube of 10 times the grain size (IG-110 = 20 μ m) results in a volume much smaller than the actual grain size. When link volumes are too small, each mesh element can end up as its own group, and the graphite behavior may be opposite how the Weibull theory works in regard to its strength dependence on volume. Figure 23 is a plot showing the full assessment POF as a function of minimum link volume and threshold for NBG-18 and a fine mesh.

Hindley [9] explains:

“The methodology is based on the hypothesis that once the material reaches a certain volume or size, the dissipation of energy between the microstructural elements is sufficient to show homogeneous mechanical rheological response in the material on a macroscopic scale. The macroscopic rheological response is measured during mechanical testing of components (tensile test, bending test etc.). The approximation of this response is achieved by a volume grouping method which defines the size of a link in the weakest link calculation. The heuristic rationale behind this is that a “link volume” is required for the material to exhibit a macroscopic rheological response. The “link volume” is proposed to be of the order of 10 times the maximum grain size (Mgs). This is proposed by Denninghoff and reported by Schmidt [29]. Ho [24] found that the grain size effect comes into existence when a tensile test specimen gauge diameter is reduced below 10 to 15 times the Mgs. Ho [24] found that the materials become far weaker when the gauge diameter is reduced to this extent.

The rationale for the formulation is that a link in the weakest link calculation should have a minimum volume to represent the macroscopic rheological response of the material. Ideally, the links should be sorted by location; however, sorting the equivalent stress intensities in order of magnitude allows for a simpler computation of the PoF. This simplification is motivated by the fact that during irradiated analysis, usually only one point of high stress occurs. If more

than one location of high stress exists, the locations would be sorted in the same group resulting in a conservative failure prediction.”

Hindley’s References:

[24]: Ho, F.H., Modified Weibull Theory for the Strength of Granular Brittle Material, G.A. Co., Editor. 1979: San Diego, CA (USA). p. 27.

[29]: Schmidt, A., Problems Connected to the Application of the Weibull Theory to the Results of a Finite Element Calculation, M. Hindley, Editor. 2007, Westinghouse Reaktor GmbH: PBMR.

5.5 V_m Sensitivity Study Results

The POF full assessment calculations were done based on 10 equally spaced threshold values from zero to just below the minimum possible threshold value (minimum observed tensile stress). Recall that the component data are subsetting, such that only component stresses exceeding the threshold are retained. For some thresholds, the subsetting results in a reduced component datasets so small that the volume grouping or stress range criteria cannot be met. In those cases, fewer points will comprise the plots, since the POF could not be calculated. An important implication of this (in terms of setting the threshold parameter) is that certain threshold parameters will not lead to a calculatable POF. For example, with graphite grade NBG-18, the minimum test specimen was 12.8 MPa. Theoretically, the threshold parameter can be any value between 0 and just under 12.8. However, with $V_m = 4.096$, only threshold values under 9 could be used to calculate the POF, per ASME-3217. As another example, for graphite grade IG-110, the maximum threshold value is just under 20.06. However, for $V_m = 0.8$ and the geometry used in this example, only threshold values under 12 can be used in the POF calculations. For all other V_m considered in this study for IG-110 (8, 80, 800), the POF calculations could only be done for a threshold of 0. For graphite grade 2114, the POF could not be calculated for any threshold/ V_m combinations, since the minimum link volume criteria was not met.

Obviously, there is an issue if the code as written cannot be used for POF calculations for some graphite grades. A few different things contribute to this. First, we must consider that the maximum reported grain size is fractional for the finer grades: 2114 and IG-110. This causes the volume based on 10 times the grain size to be less than the grain size, and smaller than most mesh elements in the meshes considered. In practical terms, the calculations do not work for finer grades. Oak Ridge National Laboratory is currently examining the dependence of volume on material strength for finer grades. Their findings suggest that the work of Ho [14] does not hold true for finer grades. Ho [14] suggests that the weakest link theory may hold for even smaller volumes of super-fine grain graphite grades. More work must be done to understand the relationship between volume and material strength for fine-grain grades of graphite so as to understand at what volume the weakest link theory no longer holds.

The second point relates to the load applied to this component. Figure 26 is a plot of six distributions. The black one is the component stress distribution. The others are the fitted Weibull lower-bound distributions of the five grades of graphite at a threshold equal to 0. This value was chosen to generate more overlap with the component stress distributions of all possible lower-bound distributions resulting from other threshold values.

We see that for the load applied to this component, PCEA has the most overlap with the component stress distribution (Figure 26). Therefore, the POF was so high for all threshold values and V_m considered. There is less overlap with NBG-17 and NBG-18, and nearly none with IG-110 and 2114. The reason the POF calculations could not be run for all but the threshold = 0 case for IG-110 and 2114 is because the resulting component volume after removing all component mesh elements with stresses less than the threshold parameter was too small to meet the minimum link volume requirement. If the component load were less, the POF for PCEA may straddle the 0.001 acceptance limit, depending on the V_m and threshold. If the component load were higher, the POF for IG-110 and 2114 may be non-zero and straddle the acceptance limit. The point is that while V_m only appears to influence the acceptance of this component when using NBG-18 material properties, this is simply due to the load applied to the component. A generalization of V_m effect on the acceptance cannot be made without considering how the POF would change as a function of component load in the FEA. The main outcome derived from this study is that the POF is lower for a larger V_m . Whether or not it is enough to affect component acceptance also depends on the threshold, mesh size, and load applied. In speaking to engineers running the FEA models, it sounds as though the load applied to the FEA modeling by vendors will be very situational and will depend on many environmental and geometric factors, and that it will be impossible to consider what load range is reasonable.

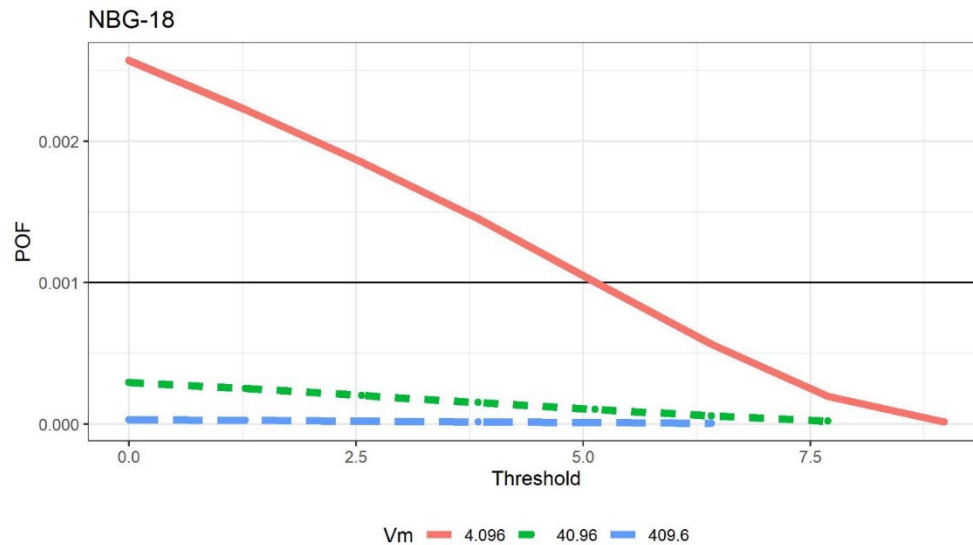


Figure 23. NBG-18: POF as a function of threshold and V_m , fine mesh.

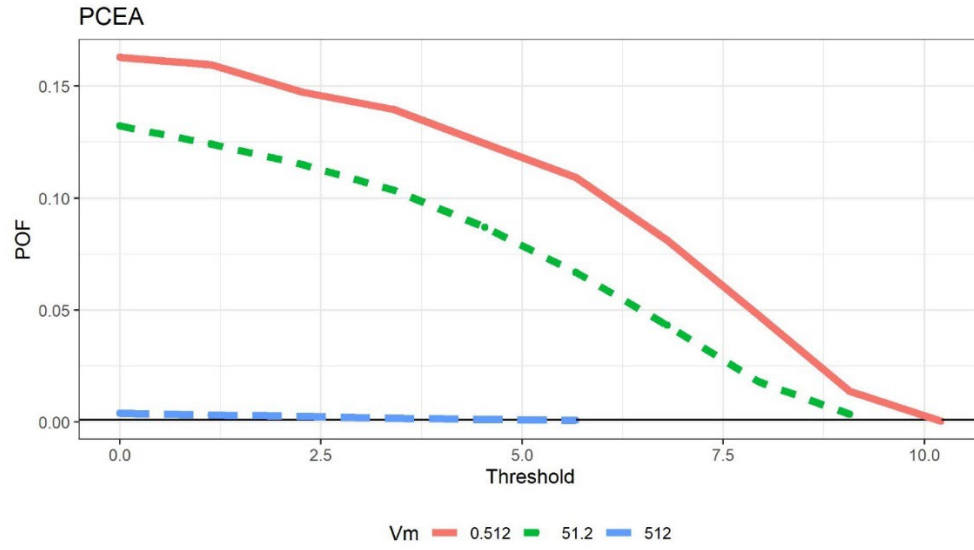


Figure 24. PCEA: POF as a function of threshold and V_m , fine mesh.

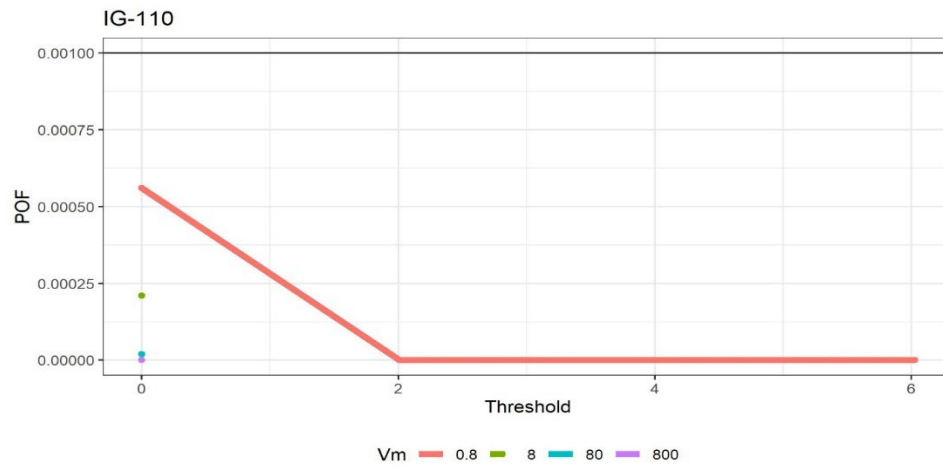


Figure 25. IG-110: POF as a function of threshold and V_m , fine mesh.

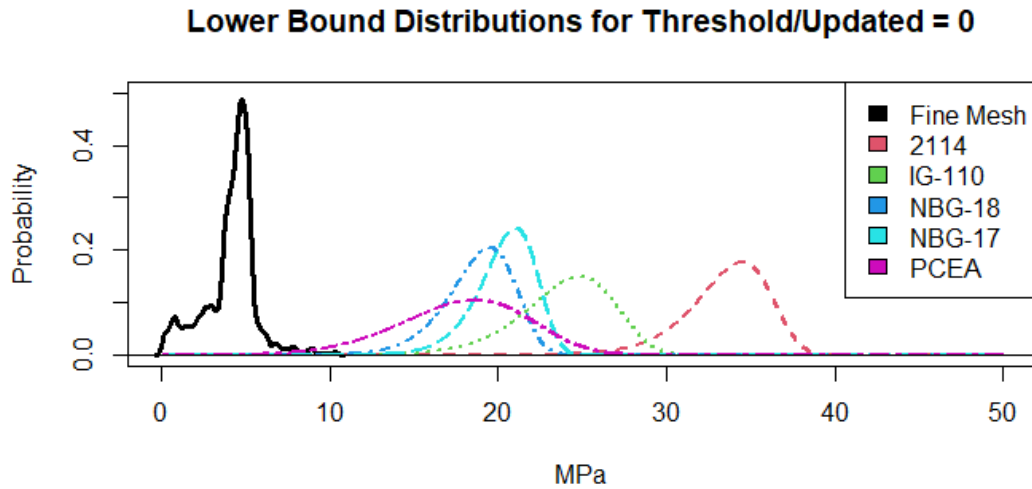


Figure 26. Comparison of lower-bound distributions used in POF calculations vs. component stress distribution for all grades of graphite.

While V_m sets the minimum link volume required for the weakest link theory to hold true for graphite, the V_m grouping criterion is only the first criterion used in the grouping step. The link volumes will have a minimum volume of V_m . However, after applying the second grouping criterion (i.e., the minimum stress range parameter), the effective link volumes will be larger.

This next case study compares the effective link volumes to the V_m , then describes the resulting effect of the stress range parameter for NBG-18. NBG-18 was chosen because the component load reflected the effect on acceptance for this grade as a function of V_m . For the first three groups, no more elements had to be added to meet the stress range criteria after meeting the minimum volume criteria. One hundred forty-nine total groups resulted from the grouping step. Figure 27 shows where the groups end, and that the groups are smaller at the beginning and end of the ordered element list (ordered by equivalent stress), with larger groups in the middle. For example: jumping to groupings toward the middle of the dataset, specifically, the group starting at element 3384, the ending element for meeting the volume grouping criterion is 3402, while the ending element for meeting both criteria is 3826. General conclusions cannot be made. What we see for this element is that the volume grouping criteria drives the group sizes at the end points, and the stress range parameter drives the group sizes in the center.

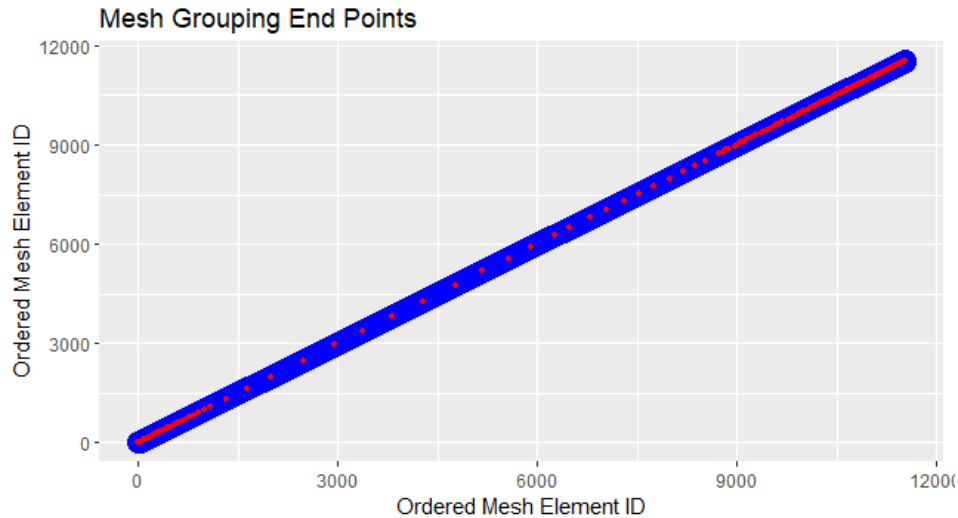


Figure 27. Comparison of group sizes in POF calculations.

While the minimum link volume and minimum stress range parameters are set for each group, the effective group volume and stress range may differ. Figure 28 and Figure 29 display the effective group volumes and stress ranges, with the red horizontal lines representing the minimum limits set by the code. The minimum link volume was set to 4.096, which is 10 times the grain size cubed for NBG-18, per the 2019 code requirement. We see that at least half the effective group volumes exceed the minimum required, with the largest being 110.424 mm³. The groups can be larger for two reasons: either the next element to be added has a much larger volume and thus pushes the total group volume over the minimum limit by a large amount, or many more elements must be added to the group to meet the stress range criteria after the volume criteria has already been met, making the effective volume much larger than required.

Weibull's weakest link theory assumes that a different failure distribution is needed for each volume, since it assumes that strength decreases with volume. This study showed that the group volumes range from 4.096 to 110.424 mm³, rather than each group having the same volume. If theoretical or experimental results show that the strength distribution of graphite does not change as a function of volume after a minimum volume of material is obtained (in this example, 4.096 mm³), then we are safe to continue using the current approach, despite the resulting range of volumes (as opposed to a single volume) in the final POF calculations. More work is needed in this area to evaluate/review the effect of volume on the strength distribution for graphite material.

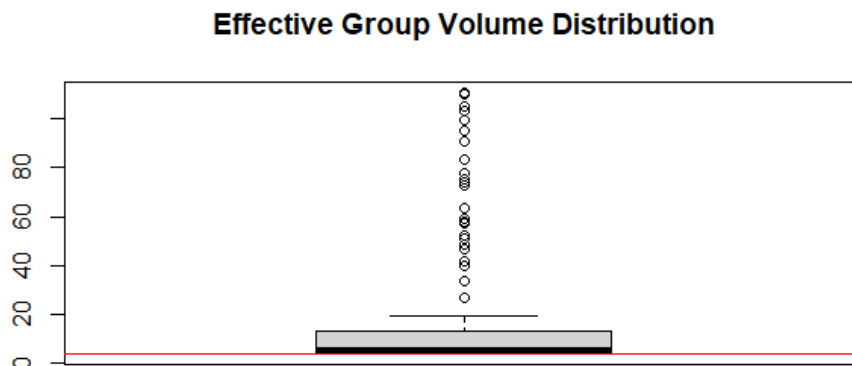


Figure 28. Boxplot of effective group volumes relative to Vm limit.

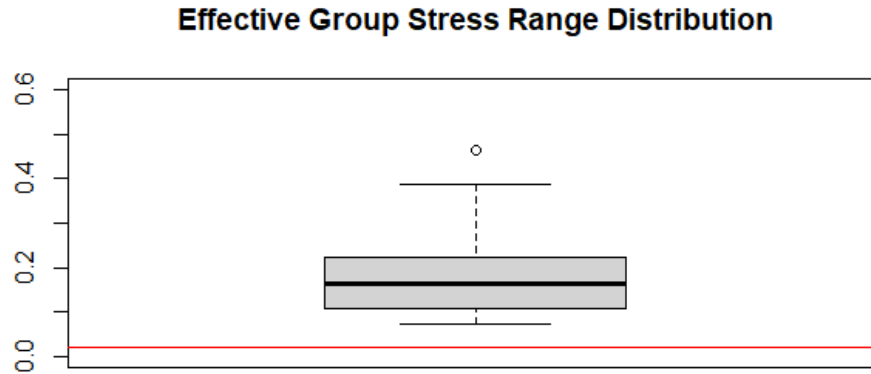


Figure 29. Boxplot of effective group relative stress ranges vs. limit.

5.6 Other Considerations

A final consideration is that the spatial aspect of the volume grouping methodology implemented in the code does not require elements that form link groups to be proximal to each other. The resulting link groupings are composed of mesh elements that are far apart spatially. However, practically speaking, it does not make sense as a methodology for determining a component POF.

6. VALIDATION

Hindley performed validation experiments to verify the POF methodology found in HHA-3217. Future work will involve similar validation experiments to inform the threshold, mesh, and volume grouping parameters. In this section, we describe Hindley’s validation approach and how it will be used and expanded moving forward.

First, Hindley explored how variable the experimental loads are expected to be when including billet-to-billet, within-billet, and orientation sources of uncertainty. He found that 50% of billets have a tensile strength within $\pm 6\%$ of the material strength average, and 95% have a tensile strength within $\pm 18\%$. This was the basis for choosing as acceptable those validation stresses that fall within 6–18% of the median experimental load.

Hindley [9] found that the highest POF was generated under the median load (50% POF). This was his justification for using the median load as the “basis for comparison.” In his thesis, he also mentions doing the study for lower POFs; however, those results were not apparent in his work. A critique of this approach is that the POFs close to the SRC acceptance criteria are much lower ($\text{POF} = 0.0001$). It is more important that the 3217 POF calculations are accurate in the left tail of the distribution rather than at the median. However, to arrive at an experimental data distribution that does a good job of characterizing the left tail of the Weibull distribution may require many test specimens. Moreover, the lower POFs are where we know the Weibull distribution does not fit well to the observed data.

Hindley’s validation method consists of the following steps:

- Find the median experimental failure load (experimental POF = 50% always)
- Apply that load to the component to generate the component stress distribution
- Use the component stress distribution in 3217 calculations to obtain a calculated POF
- Find the difference between the calculated and experimental POFs
- Scale the component stresses by this difference

- Recalculate the POF
- Repeat until convergence
- Compare the average component stress that resulted in a calculated POF of 50% against the median experimental load.

Table 5 below summarizes the results from Hindley's and Robert's validation experiments. The tables include the geometries, their variations, the tests performed, the number of test specimens, and the results. In Hindley's results (Table 7-3 in his thesis), he shows multiple data points for each test case. It is unclear how the test specimens were allocated to arrive at fewer data points. The colors help indicate how the majority of the data points performed in the calculated median load relative to the experimental median load. Green indicates that the majority of the points were within 50% variation, yellow indicates they were within 95% variation, and dark orange indicates they were outside the limits.

Table 5. Table of previous validation work.

Test	tensile (VP-00)		compressive (VP-19)		4-point bend (VP-01)	
Geometry	dog bone		cylinder	cubic	cylinder	
Variations	end loaded	clamped			experiment	extended
Median Experimental / Calculated Load	6.5/6.52 kN	6.5/6.52 kN	24.91/24.66 kN	33.74/31.39 kN	2.69/2.44 kN	
# Reported Data Points	3	3	2	2	2	1
Total Reported Tests	370		262		260	
Paper Author	Hindley		Hindley		Hindley	

Test	4-point bend (VP-12) continued							
Geometry	Notched Bar, Notch Up				Notched Bar, Notch Down			
Variations	1mm	5mm	10mm	20mm	1mm	5mm	10mm	20mm
Median Experimental / Calculated Load	4.43/3.9 1 kN	4.17/3.73 kN	4.08/3.57 kN	3.91/3.39 kN	2.36/1.68 kN	2.86/2.45 kN	3.09/2.68 kN	3.37/2.83 kN
# Reported Data Points	3	3	3	3	3	3	3	3
Total Reported Tests	160 - 10 per geometry variation							
Paper Author	Hindley							

Test	4-point bend (VP-12)							
Geometry	Dog Bone, Across Thickness				Dog Bone, Across Width			
Variations	1mm	5mm	10mm	20mm	1mm	5mm	10mm	20mm
Median Experimental / Calculated Load	9.66/8.58 kN	10.25/9.58 kN	10.99/9.97 kN	11.26/10.49 kN	7.10/5.17 kN	7.65/6.20 kN	8.01/6.55 kN	8.57/6.95 kN
# Reported Data Points	3	3	3	3	3	3	3	3
Total Reported Tests	160 - 10 per geometry variation							
Paper Author	Hindley							

Test	sleeve burst (VP-15)	tensile (VP-17)	compressive (VP-17)	multi-axial fatigue (VP-18)	
Geometry	not specified	dog bone	dog bone	door knob cover (disc)	
Variations				internal pressure	external pressure
Median Experimental / Calculated Load	2.69/2.05 MPa	2.64/2.67 kN	11.23/10.10 kN	10.14/2.03 MPa	34.82/5.09 MPa
# Reported Data Points	2	2	2	3	3
Total Reported Tests	6	unknown	unknown	unknown	unknown
Paper Author	Hindley	Roberts	Roberts	Roberts	Roberts

This information can be used to some degree in performing future validation tests. Limitations include:

- Specimen dimensions are not provided for all tests.
- It is unknown where the load is applied.
- Only the mean of the experimental data is provided. Therefore, the distribution of experimental stresses is unknown.
- Hindley says the validation was done at lower left tail quantiles, but those results are not reported. Without the entire data distribution, the left tail of the distribution (which is of the most importance) cannot be validated.
- The experiments were only conducted on one grade of graphite.

The proposal for future validation experiments is to address these limitations. As background, it is helpful to understand that tensile stress tests should always perform perfectly, because tensile material data are used in the code. When Hindley's results show the other tests performing poorly in terms of validation, this is likely due to the stress magnitude differences between the experimental data (with various test types) and material data (always uses a tensile test).

Future work will expand on the work done by Hindley, and will include multiple graphite grades, with emphasis on fine-grain grades. Multiple test specimens will be tested for each geometry and grade. If possible, inter-lab variabilities will be estimated. Additionally, more attention will be paid to the left tail of the distribution during validation efforts. However, this will be a challenge limited by the number of samples reasonable.

7. REFERENCES

1. Casella, G. & Berger, R. 2002. *Statistical Inference*, 2nd Edition. Published by Wadsworth.
2. Weibull, W. 1939. A statistical theory of strength of materials. *IVB-Handl*.
3. Quinn JB, Quinn GD. 2010. A practical and systematic review of Weibull statistics for reporting strengths of dental materials. *Dent Mater*. doi: 10.1016/j.dental.2009.09.006. Epub 2009 Nov 28. PMID: 19945745; PMCID: PMC3086645.
4. National Institute of Standards and Technology (NIST) Engineering Statistics Handbook (online), version 2022. <https://www.itl.nist.gov/div898/handbook/apr/section1/apr162.htm>.
5. ASTM D7846-21, 2021. "Standard Practice for Reporting Uniaxial Strength Data and Estimating Weibull Distribution Parameters for Advanced Graphites."
6. Thoman, D. R., Bain, L. J., and Antler, C. E. 1970. "Maximum likelihood estimation, exact confidence intervals for reliability, and tolerance limits in the Weibull distribution," *Technometrics*, 12:2, 363-371. <https://www.tandfonline.com/doi/abs/10.1080/00401706.1970.10488674>.
7. Evans, J. W., Kretschmann, D. E., and Green D. W. 2019. *Procedures for Estimation of Weibull Parameters*. General Technical Report FPL–GTR–264. Madison, WI: U.S. Department of Agriculture, Forest Service, Forest Products Laboratory. https://www.fpl.fs.fed.us/documnts/fplgtr/fpl_gtr264.pdf.

-
- 8 R Core Team. 2021. R: A language and environment for statistical computing. R Foundation for Statistical Computing, Vienna, Austria. <https://www.R-project.org/>.
 9. Hindley, M. P., 2015 *Next generation high-temperature gas reactors: A failure methodology for the design of nuclear graphite components*. Dissertation. <https://scholar.sun.ac.za/handle/10019.1/97071>.
 10. Duffy, S. F. and Parikh, A. 2014 “Quality Control Using Inferential Statistics in Weibull-based Reliability Analyses,” Graphite Testing for Nuclear Applications: The Significance of Test Specimen Volume and Geometry and the Statistical Significance of Test Specimen Population, STP 1578, Nassia Tzelepi and Mark Carroll, pp. 1–18, doi: 10.1520/STP157820130122.
 11. Heo, J. H., Salas, J. D., and Kim, K. D., 2001. “Estimation of confidence intervals of quantiles for the Weibull distribution.” *Stochastic Environmental Research and Risk Assessment* 15 284-309.
 12. Meeker, W. Q. and Escobar, L. A. 1998. *Statistical methods for reliability data*, New York: Wiley series in probability and statistics.
 13. Burchell, T. D., Erdman, III, D. L., Lowden, R. R., Hunter, J. A., and Hannel, C. C. 2017. “The Fracture Toughness of Nuclear Graphites Grades.” <https://info.ornl.gov/sites/publications/files/Pub71614.pdf>.
 14. Ho, F. H. 1979. *Modified Weibull Theory for the Strength of Granular Brittle Material*, G.A. Co., Editor. San Diego, CA (USA). p. 27.